

**Mechanical Engineering Note – Safety
Analysis of Molten Uranium/Water
Interaction in the Uranium Foundry
Furnace**

J. Sze

August 19, 1993

U.S. Department of Energy

Lawrence
Livermore
National
Laboratory

DISCLAIMER

This document was prepared as an account of work sponsored by an agency of the United States Government. Neither the United States Government nor the University of California nor any of their employees, makes any warranty, express or implied, or assumes any legal liability or responsibility for the accuracy, completeness, or usefulness of any information, apparatus, product, or process disclosed, or represents that its use would not infringe privately owned rights. Reference herein to any specific commercial product, process, or service by trade name, trademark, manufacturer, or otherwise, does not necessarily constitute or imply its endorsement, recommendation, or favoring by the United States Government or the University of California. The views and opinions of authors expressed herein do not necessarily state or reflect those of the United States Government or the University of California, and shall not be used for advertising or product endorsement purposes.

This report has been reproduced
directly from the best available copy.

Available to DOE and DOE contractors from the
Office of Scientific and Technical Information
P.O. Box 62, Oak Ridge, TN 37831
Prices available from (615) 576-8401, FTS 626-8401

Available to the public from the
National Technical Information Service
U.S. Department of Commerce
5285 Port Royal Rd.,
Springfield, VA 22161



4AN93-103597-00

Mechanical Engineering Note

**Safety Analysis of Molten Uranium/Water Interaction
in the Uranium Foundry Furnace**

By

John Sze

August 19, 1993

Prepared by:

John Sze, Device Engineer
Defense Technologies Engineering Division

Approved by:

Larry E. Sedlacek, Group Leader
Defense Technologies Engineering Division

Reviewed by:

Robert E. Clough, Division Leader
Defense Technologies Engineering Division

JS:pm

Distribution:

A. Lingenfelter, L-350
L. Sedlacek, L-122
J. Sze, L-122
R. Clough, L-125
Eng. Information Center, L-127

TABLE OF CONTENTS

Section	Page
1.0 Scope	3
2.0 System Description	3
3.0 Hazards.....	8
4.0 Summary	8
5.0 Design Analysis	9
5.1 Molten Uranium/Water Interaction	9
5.2 System Response	12
6.0 Equipment Description	14
7.0 Reference	22
Appendix A.....	23
Appendix B	80

1.0 Scope

This Engineering Note describes the development of the accident criteria used the basis for the design of the uranium foundry vacuum vessel. The results of this analysis provide input into other safety notes that investigate how well the uranium containment boundary will maintain its integrity during the design basis accident. The preventative measures that have been designed into the system to minimize the potential to produce a flammable gas mixture are described. The system response is designed for consistency with applicable sections of the LLNL Health and Safety Manual, as well as the Mechanical engineering Safety Design Standards.

2.0 System Description

The uranium foundry is located in Building 231, Room 1956A. The floor plan of the foundry is shown in Fig. 1. The vacuum furnace and the assembly hood is shown in Fig. 2. The casting module showing the orientation of the crucible and the mold inside the furnace is shown in Fig. 3. A schematic of the furnace assembly and other equipment in the foundry is illustrated in Fig. 4 and a list of the foundry design parameters is given in Table 1. The vacuum furnace is designed to melt up to 100 kg of uranium alloy in an induction heated crucible and subsequently drain into an induction heated mold beneath the crucible. There are two induction power supplies in the foundry, one for melting materials and the other for mold heating. The design also includes two water cooling systems. An open loop system is used for chamber wall, power supplies and bus bars cooling and a closed loop system is used for cooling chamber internal hardware. The vacuum furnace and the assembly hood are designed to be vented into a 3000 cfm HEPA filtration negative air system before releasing the exhaust into the atmosphere.

TABLE 1
Uranium Foundry Parameter List

1. Vacuum Vessel

- | | |
|--------------------|--------------------------------|
| • Chamber Size | 36" x 36" x 60" H (Inside) |
| • Chamber Material | 1.00" THK. 304 Stainless Steel |
| • Chamber Weight | Approx. 5000 lbs |

2. Operating Conditions

- | | |
|-----------------------------|------------------------|
| • Uranium Charge Capacity | 100 kg maximum |
| • Uranium Melt temperature | ~ 1500°C |
| • Mold Temperature | Approx. 700°C - 1000°C |
| • Crucible Input Power | 100 kW maximum @ 3 kHz |
| • Mold Input Power | 30 kW maximum @ 50 kHz |
| • Vessel Internal Pressure | 10 ⁻⁶ Torr |
| • Cooling Water Temperature | 50°C maximum |
| • Cooling Water Pressure | 45 psig maximum |
| • Cooling Water flow | 25 gpm maximum |

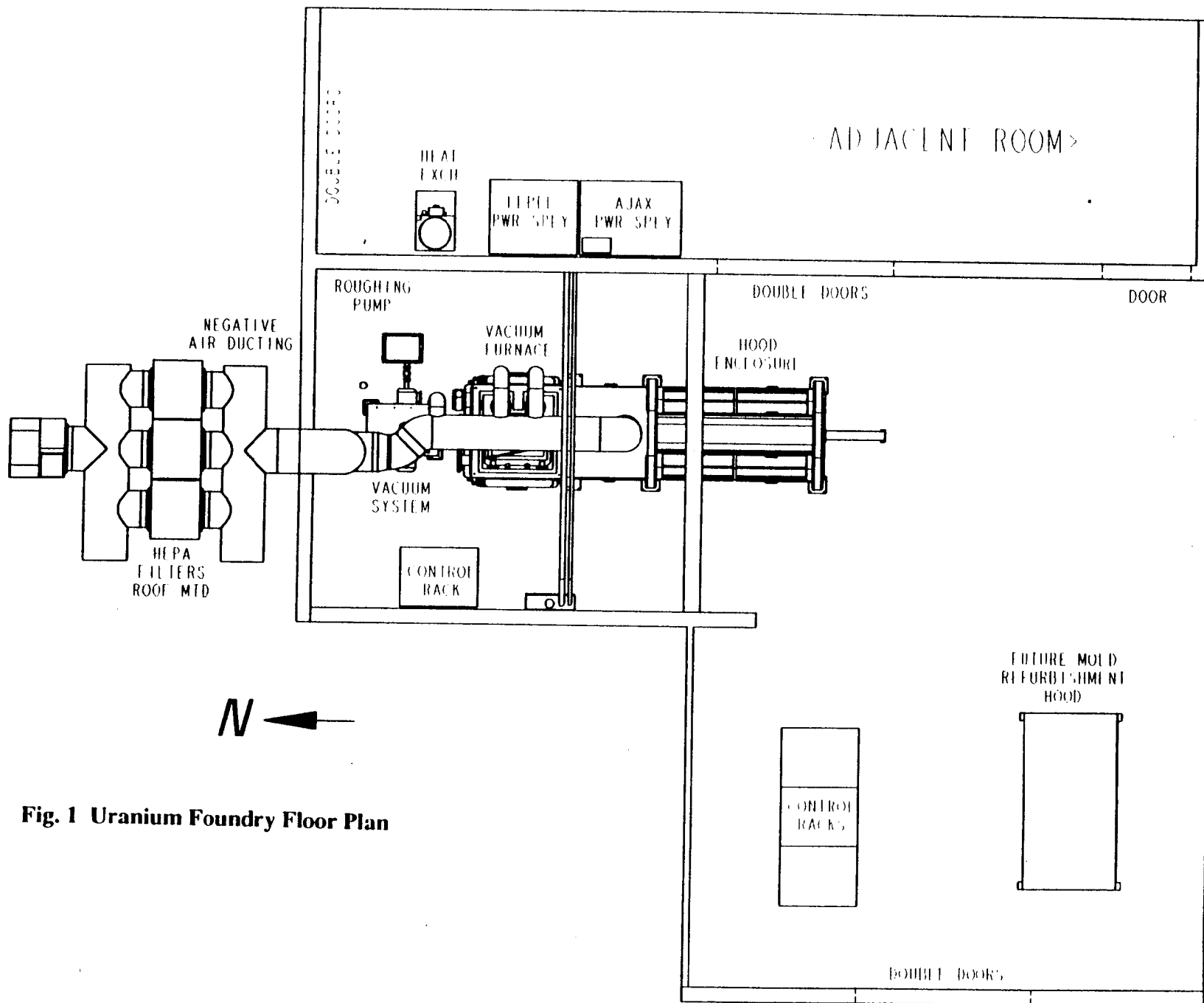


Fig. 1 Uranium Foundry Floor Plan

8/12/93

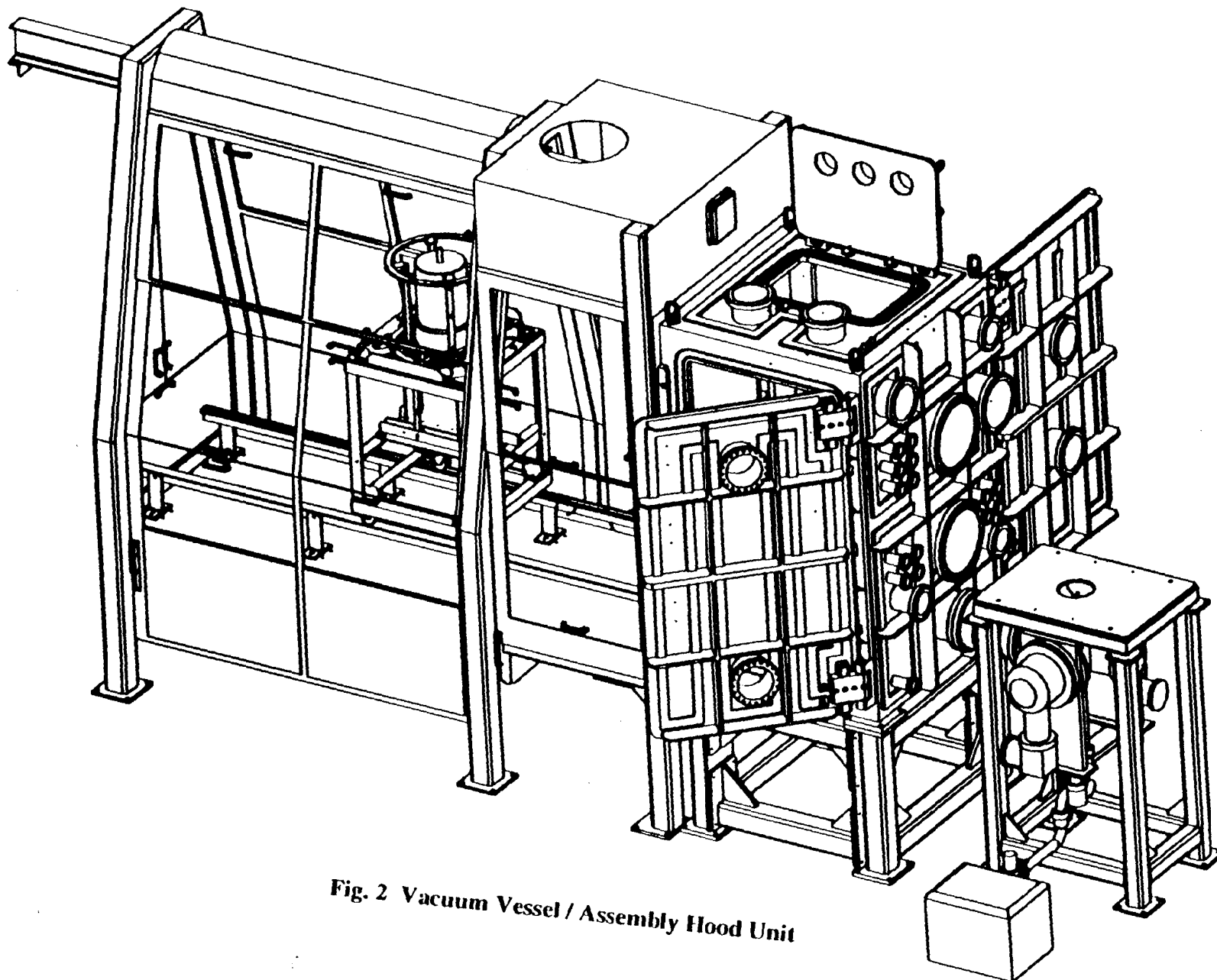


Fig. 2 Vacuum Vessel / Assembly Hood Unit

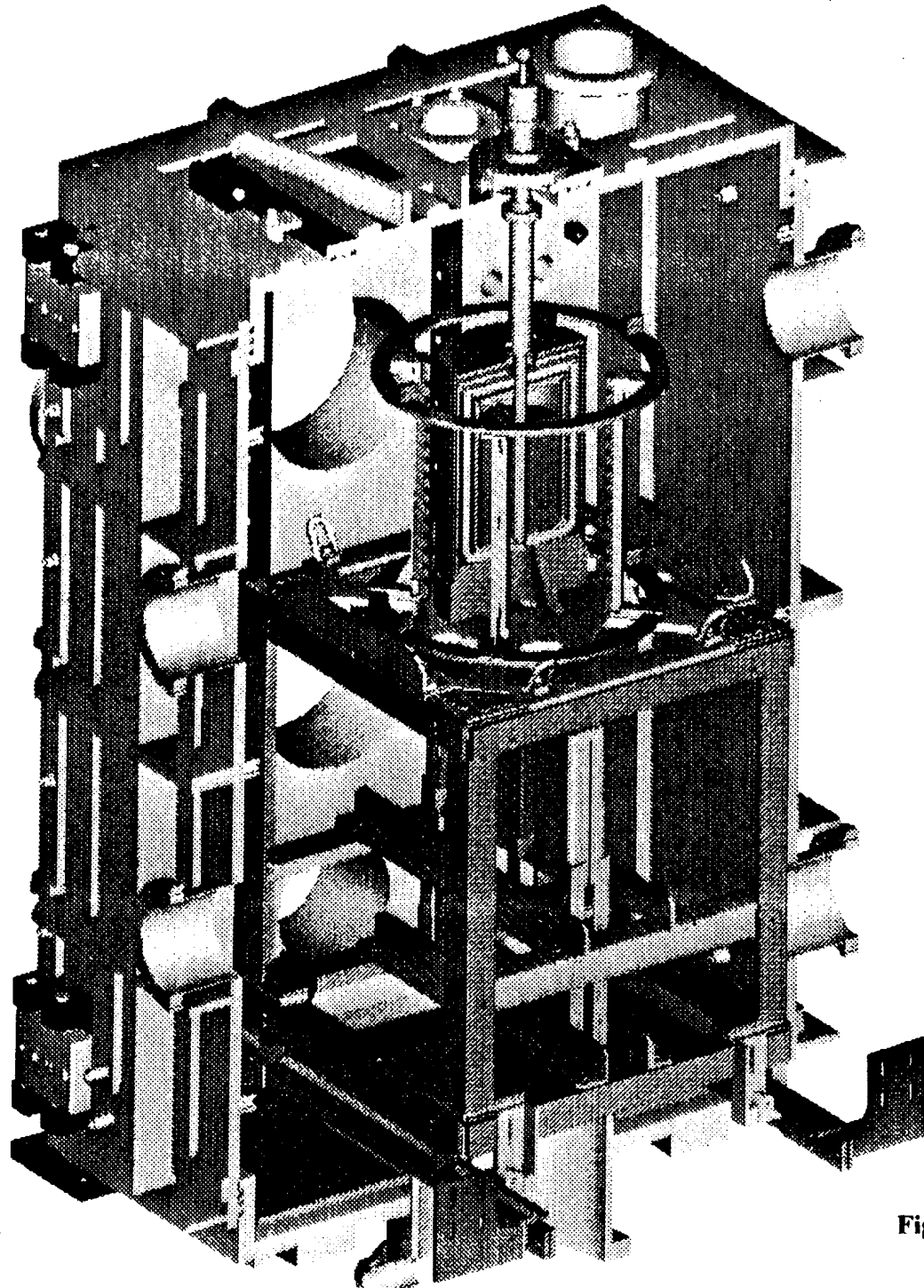


Fig. 3 Casting assembly

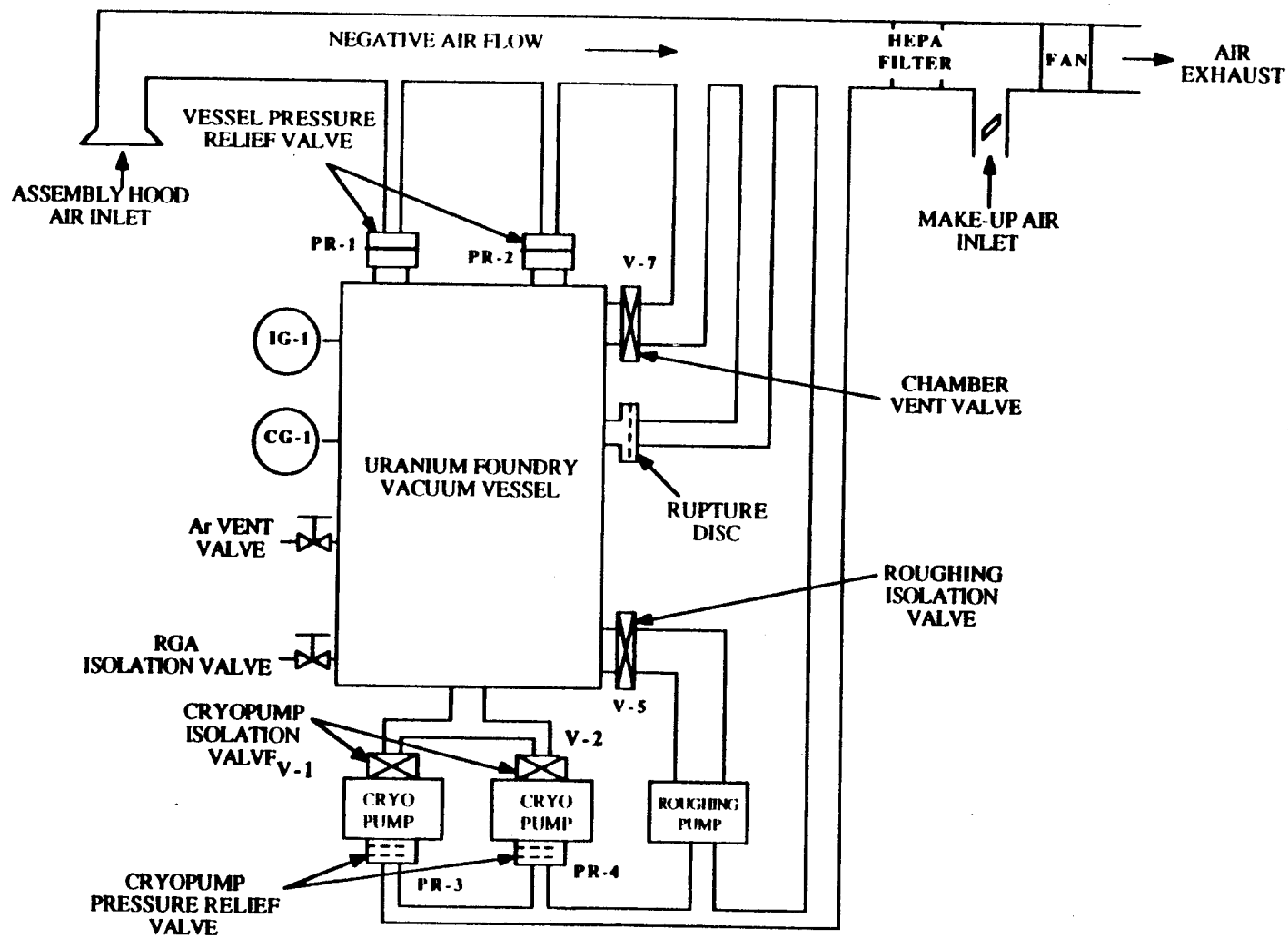


Fig. 4. Schematic of uranium foundry furnace and other equipment

3.0 Hazards

This analysis investigates the following possible hazards associated with molten metal and water interaction in the vacuum vessel.

- Steam generation leading to over pressure
- Hydrogen deflagration
- Damaging steam explosion pressures
- Thermal melt through of vacuum vessel floor

4.0 Summary

The safety philosophy in the furnace design is to limit the amount of water available to participate in a molten uranium/water interaction by isolating the coolant flow when an accident condition is detected. The safety analysis (see Appendix A) concluded that hydrogen deflagration and damaging shock pressures resulting from the interaction between molten uranium (~ 1500°C) and water can be ruled out due to lack of sufficient premixing between the molten metal and water. The maximum pressure in the vessel from a worst case accident scenario has been calculated to be less than 15 psig over pressure with proper venting capability. This is a conservative estimate because the condensing capability of the vessel wall has been ignored. The vessel is designed to withstand a 15 psig over pressure. Hence, even in the worst case accident condition, the vacuum vessel will not fail.

The primary system response to a water leak inside the vacuum vessel is that the roughing pump isolation valve opens when the vessel pressure rises above the setpoint, pumping steam and hydrogen out of the vessel. The roughing pump remains on during a run and quickly provides a pumping capacity of 3200 cfm to vent the vessel into the negative air duct.

Even if the primary system response fails, the vessel will not pressurize because of the two pressure relief valves and the rupture disc. These two backup systems preserve the structure integrity of the vessel and allow the steam and hydrogen to vent into the negative air duct in a safe manner.

The potential of thermal melt-through due to the accumulation of the molten uranium (~100 kg) on the vessel floor can be ruled out. The calculation shows that the vessel floor temperature will rise to ~ 230°C, it is well below the eutectic temperature for the uranium metal-steel system.

5.0 Design Analysis

The design analysis address two aspects of water leak inside the vacuum vessel: the potential consequences of molten uranium and water interaction, and the system response. The design analysis has been review by an independent consultant, Charles Landram, who is a thermal/fluid specialist in the NTED Division of Mechanical Engineering Department. The Potential consequences of molten uranium and water interaction in this furnace was conducted by Fauske and Associates, Incorporated, The analysis assumes the roughing pump fails to pump hydrogen and steam out of the vessel, resulting in a conservative estimate of the steam and hydrogen generation rates and inventories. The full report is included as Appendix A. The system response to a water leak is described in Section 5.2.

5.1 Molten Uranium/Water Interaction

In this analysis there are two accident scenarios leading to molten uranium and water interaction were considered:

1. Rupture of crucible resulting in the melt contacting the water cooled induction coil.
2. Accumulation of water in the mold or chamber floor and subsequent release of molten uranium.

Typically, only one of these systems would be anticipated to fail, but a conservative approach was considered and the key assumptions are summarized below:

- a. All of the water coils were assumed to be broken with all the water available in the closed loop system (~10 gal.) spilled onto the vacuum chamber floor.
- b. The crucible was assumed to be broken with 100 kg of molten uranium at 1500°C available to burn through a cooling coil or to interact with water accumulated on the chamber floor.
- c. Along with the above conditions, the vacuum boundary could be broken and air could enter into the furnace.
- d. The vessel volume is 1.27m³ (i.e. the vessel isolation valves are closed) and the flow area through the pressure relief valves is 0.034m². The pressure relief valves are assumed to be the only flow exit, and open when the vessel pressure reaches approximately 1.0 psig.
- e. The experimental data developed by the nuclear industry (see Appendix A, Section 3) shows the heat flux for molten uranium dropped into a pool of water could be as high as 10 to 30 MW/m² for a short time (< 10 s). The projected area of the chamber floor was used as the pertinent value for determining the total energy production rate.
- f. Maximum steam generation rate was assumed to be limited by the ability of the water droplets to remain as part of the co-dispersed medium.
- g. Due to the shallow layers of water (0.045m) on the chamber floor not allowing the necessary pre-mixing configuration to be established between the molten uranium and water, Fauske concluded that any energetic steam

explosive events can be ruled out. Instead a configuration consisting initially of a molten uranium metal layer and a water layer separated by a steam blanket would likely develop.

- h. At the lower bound steaming rate (0.26kg/s), there will be sufficient steam inerting taking place in the vacuum vessel for the postulated accident scenarios to eliminate the potential for hydrogen deflagration.
- i. The accumulation of the entire uranium inventory of 100 kg on the chamber floor would not lead to thermal melt through. Charles Landram calculated the vessel floor temperature will rise to $\sim 230^{\circ}\text{C}$, it is always well below the 800°C eutectic temperature for the uranium metal-steel system[1].
- j. Based on the maximum steaming rate (11 kg/s) the relief area of about 0.033 m^2 or two 6 inch ports would be adequate without causing the vessel pressure buildup to exceed 15 psig. The analysis suggests that the opening pressure for the relief system should be set near ambient pressure (~ 1 psig) to allow for the maximum time (~ 0.1 s) to assure a fully open relief system as the pressure approaches the chamber design pressure of 15 psig. If any one of the pressure relief valves malfunction and the vessel reaches pressure $13 \text{ psig} \pm 2 \text{ psig}$, an 8 inch rupture disc will burst to vent the vessel into the negative air system.

The vessel pressure is shown as a function of time for the worst case scenario (i.e., roughing pump fails) in Fig. 5. The steam pressure builds up because water is in contact with surface temperature well above the boiling point with a steaming rate of 11 kg/s. Steam generation continues after the relief valves open at its cracking pressure of ~ 1.0 psig to vent gas into the negative air duct. The vessel pressure continues to build up and reaches a maximum pressure of ~ 9.7 psig in about 0.06 s after the relief valves open. The vessel venting rate increases with the venting area of the relief valve which causes the vessel pressure to decrease. This is a very conservative assumption because the condensing capability of the vessel wall has been ignored and the roughing pump will normally be on during a water leak. Hence the implicit assumption is that the roughing pump fail at the same time the water leak occurs.

- k. The cooling coil will not be damaged by direct contact of molten uranium because of the uranium crust formation on the copper surface as concluded by Fauske (see Appendix A, Section 2). This accident scenario was also analyzed by Charles Landram [1] independently with different assumptions and his calculation showed that the copper cooling line is likely to be ruptured by thermal melt-through. Nevertheless, a cooling line failure poses no additional impact with respect to safety issue of the vessel design (see Appendix B).

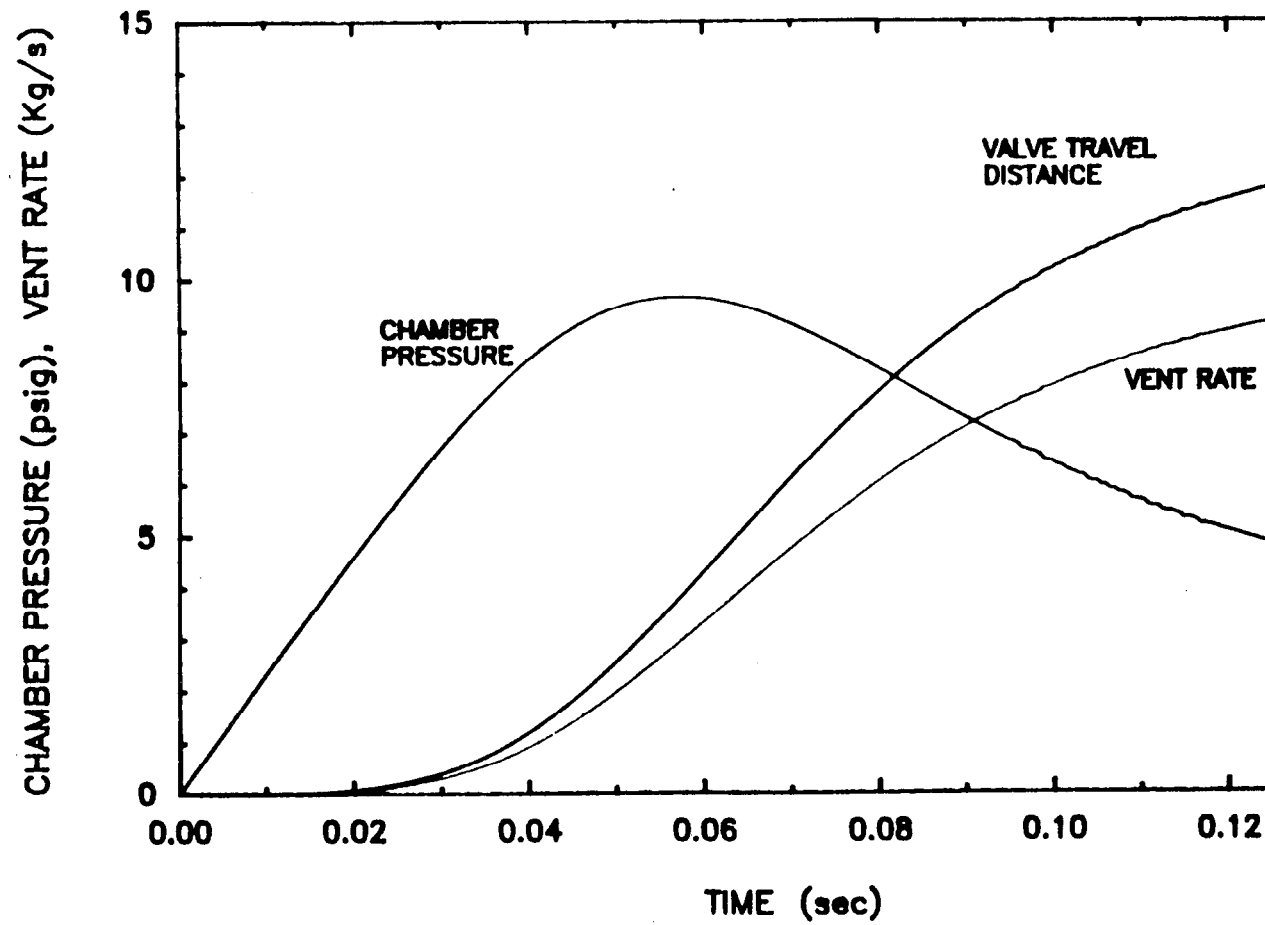


Fig. 5. Calculated chamber pressure relief capability as a function of tim

5.2 System Response

The Primary system response to a water leak occurs inside the vessel and is provided by the operation of the roughing pump, which will maintain a low hydrogen and steam inventory in the vessel. If the primary response is defeated the system has two back up responses. The first back up is to vent the chamber using two pressure relief valves. If either or both of the pressure relief valves malfunction, the second back up is to vent the chamber through a rupture disc. The details of the system response to a chamber over pressure are shown in Fig. 6, and described below.

- a. Ion pressure gauge, IG-1 (see Fig. 4), inside the vessel sense a pressure rise from the normal operating pressure of $<10^{-5}$ Torr. If the pressure rises to greater than 6×10^{-4} Torr, the control system automatically shuts off the induction power supplies, closes the cryopump isolation valves V-1 and V-2 and sends an alarm to the operator.
- b. If the pressure rise sensed by the convectron gauge, CG-1, is below 30 mTorr, the operator may reopen the high vacuum isolation valves (V-1 and V-2) in an attempt to continue operation. If the pressure is reduced to 10^{-6} Torr range by this action then the induction power supplies can be manually turned back on. If the pressure is not reduced to 10^{-6} Torr range, the operator must identify the gas source or terminate the run.
- c. If the convectron gauge, CG-1, reports a pressure rise greater than 30 mTorr, the control system automatically opens the roughing isolation valve V-5, allowing the roughing system to pump on the vessel. If the pressure stabilizes below 30 mTorr, then the operator may attempt to cross back over to high vacuum. When the convectron gage senses chamber pressure greater than 1 mTorr the ion gauge shuts off independently of the control system as well as closes the RGA isolation valve to protect equipment and to eliminate a possible ignition source.
- d. The roughing pump has a capacity of 3200 cfm and the pump exhaust is connected to the negative air system to prevent the possibility of releasing any contaminant into the atmosphere. The worst case scenario described in Section 5.1 will only occur if the rough pump fail to pump the vessel.
- e. If the convectron gauge CG-1 indicates the chamber pressure ≥ 20 Torr and the flow sensor indicates a decrease of coolant flow below the setpoint, then the system response as if there is a major water leak inside the chamber. The control system then automatically closes both inlet and outlet control valves of that cooling loop to minimize water egress into the chamber and sends an alarm signal to the operator. Water in other cooling loops continues to flow. The objective of this action is to limit the amount of water available to potentially react with molten uranium. If the solenoid valves fail to stop the cooling water, the operator can manually close two ball valves to shutoff the water flow.

Each cooling loop has two water pressure relief valves for redundancy to prevent over pressure in the cooling lines. If the cooling line pressure buildup to 150 psig or 210°F, the pressure relief valve will vent the line pressure into the closed loop water tank.

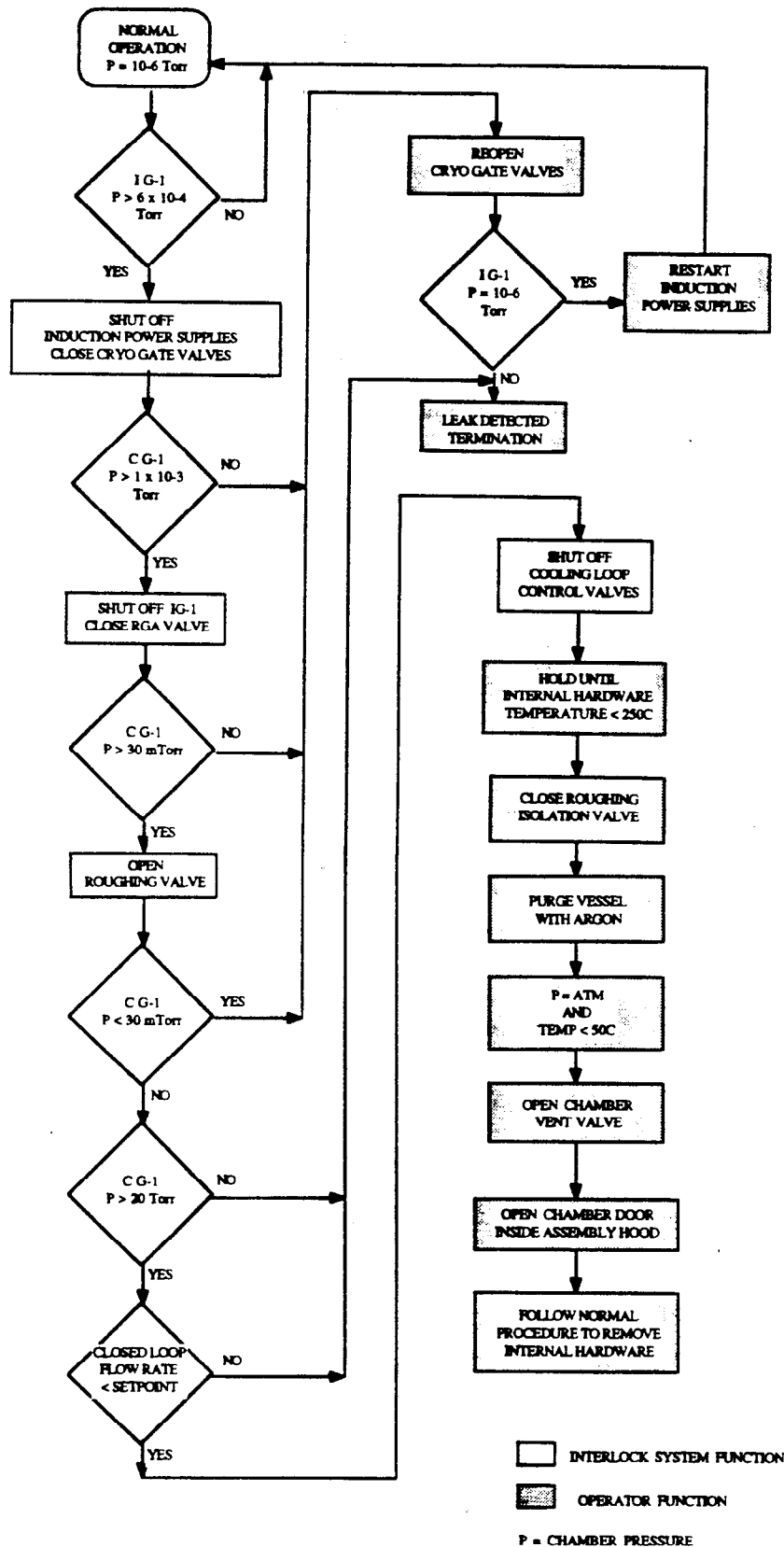


Fig. 6. System response to a water leak flow diagram

- f. After the internal hardware temperature decreases to less than 250°C, the roughing isolation valve V-5 is closed. Argon gas is available to bleed into the vessel. The argon gas is used to purge the vessel if the roughing pump failed and substantial pressure built up in the vessel while the internal hardware was hot. The argon line has a 3 psig pressure relief device to prevent over pressurization of the vessel during venting.
- g. After the internal hardware has cooled to ~50°C and the roughing isolation valve is closed, the argon vent valve can be opened by operator command. When the vessel pressure reaches atmospheric, chamber vent valve V-7 is opened to provide flow to the HEPA filters. The chamber door inside the assembly hood can be opened and the internal hardware removed following the usual procedures.

6.0 Equipment Description

The equipment described below is designed to satisfy the design analysis.

Roughing Pump: Vessel roughing is provided by an oil-free mechanical pump located inside the experimental area. The pumping capacity is 3200 cfm. During normal operation, the roughing pump is used to pump the vessel down to 10 to 50 mTorr range before switching over to high vacuum. The pump is connected to the vessel with a 2 inch vacuum line. The exhaust of the roughing pump is connected to the negative air duct with a 3 inch line.

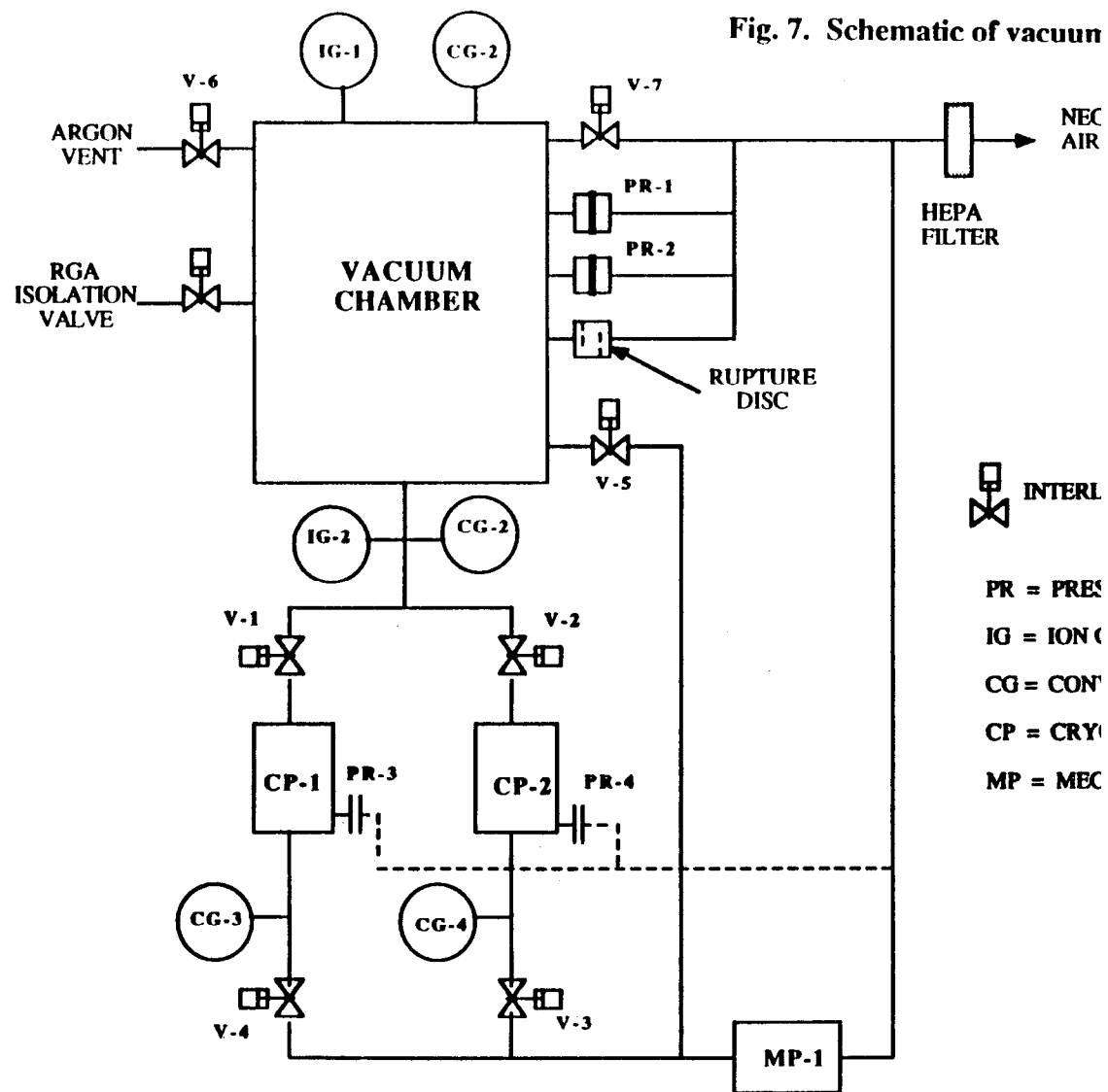
During a water leak the primary system response to a water leak is to pump hydrogen and steam out of the vessel as it is being generated. The pump will minimize the accumulation of hydrogen inside the vessel, and prevent the vessel from venting into the negative air duct

High Vacuum: A schematic of the vacuum system is shown in Fig. 7. Cross over to the high vacuum pumps occurs when the vessel pressure is reduced to below 30 mTorr. Isolation valve V-5 is closed, but the roughing pump remains on. Two gate valves V-1 and V-2 are opened and the vessel is pumped down to a pressure below 10^{-6} Torr by two cryopumps. The pumping speed and the capacity are listed in Table 2. However, the pumping capacity of the high vacuum pumps is not a factor in the event of a water leak because the valves to the cryopumps automatically close once the operating pressure is exceeded. The pressure relief vent at the cold head of the cryopump is connected to the negative air duct to eliminate the possibility of releasing hydrogen or contaminant into the experimental area.

TABLE 2

Cryopump CRYO-TORR 8F Specifications

1. Pumping Speed		
H ₂ O	4000	1 / sec
Air	1500	1 / sec
Argon	1200	1 / sec
H ₂	2200	1 / sec
2. Pumping Capacity		
Argon	1000 std. liters	
Hydrogen at 5×10^{-6} Torr	8 std. liters	



Negative Air: A negative air fan and three HEPA filters provide negative air pressure to the vacuum vessel as well as the assembly hood. The specification drawing of the negative air system is shown in Fig. 8. The capacity of the negative air fan is ~3000 cfm. A 14 inch diameter sheet metal duct leads from the vessel and the assembly hood to the HEPA filters on the roof of Building 231. The ducting is rated to be operated at a negative pressure of 7 inch of water (0.25 psi) and the assembly hood is rated to be operated at a negative pressure of 10 inch of water (0.36 psi). A separate control system (see Fig. 9) is used to provide negative air flow with face velocity of $125 \text{ fpm} \pm 25 \text{ fpm}$ at the assembly hood to comply with the LLNL Health & Safety Standards [4]. The performance of the HEPA filtration system is monitored continuously. Visual and audio warning signals will be given to the operator if the performance of the filtration system drop below the operating setpoint. In the event of the accident scenario as described in section 5.1, the gas flow into the duct is not flammable under any conditions, and hence will not burn the HEPA filters.

Chamber Vent Valve: Under normal operating conditions, a 6 inch chamber vent valve V-7 (see Fig. 10) can be opened by operator command after a casting run. When the chamber pressure reaches atmospheric, the valve is opened to provide flow to the HEPA filters, then the vessel door located inside the assembly hood can be opened. Air may enter into the vessel during the opening of the vessel door and may cause portions of the exposed uranium to oxidize. The reaction rate is controlled by introducing air slowly after the internal hardware has cooled to below 50°C and the amount of Argon present inside the vessel.

Pressure Relief Valve: The two 6 inch pressure relief valves PR-1 and PR-2 located on the top of the vessel (see Fig. 10) limit the maximum pressure in the vessel to below 10 psig, depending on the final valve calibration. The relief pressure for these two valves is set at approximately 1.0 psig. These valves vent into the negative air duct, by-passing the chamber vent valve V-7 between the negative air duct and the vessel. The pressure relief valve is described in detail in [2].

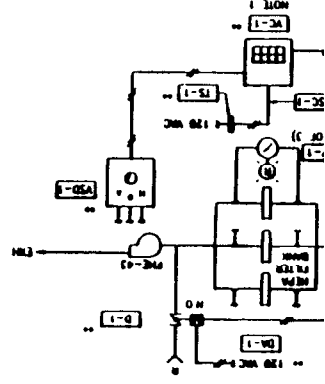
The pressure relief valves provide the secondary system response to a water leak. If the roughing pump fails, the vessel pressure is limited by the relief valves. The vessel with all its instrumentation and feed-thrus will be tested to 15 psig, which is 1.5 times the expected maximum chamber pressure, to insure containment is maintained.

Rupture Disc: A rupture disc located on the side of the vessel (see Fig. 10) limits the maximum over pressure in the vessel to less than 15 psig. The rupture disc provides the second backup system response to a water leak. If both the roughing pump and the pressure relief valve fail, the disc bursts allowing the vessel to vent into the negative air duct by-passing both pressure relief valves and the chamber vent valve. The rupture disc is designed, built and certified by the disc manufacturer to operate in vacuum below 10^{-6} Torr and to burst at $13 \text{ psig} \pm 2 \text{ psig}$.

Cooling Water: There is a single closed loop heat exchanger and pump unit which provides three closed loop water cooling systems inside the vessel (see Fig. 11). One for the crucible induction heating coil, the second for the mold induction heating coil and the third for the active mold temperature control. The closed loop cooling system provides up to 25 gpm at 45 psig to the vessel during normal operation. Since these cooling lines could develop leaks either due to extended use, or as the result of an accident condition,

Fig. 8. Negative air system specification drawing

OP CONTROL LAYOUT



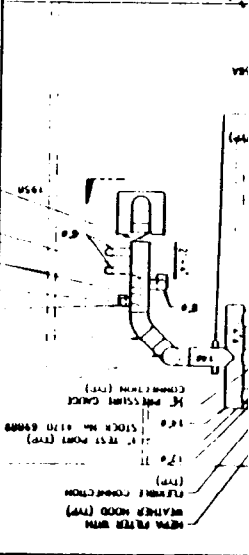
NOTES:
1. CONTROL CONNECTIONS SHALL BE MADE BY THE CONTRACTOR.
2. CONTROL CONNECTIONS SHALL BE MADE BY THE CONTRACTOR.

SEQUENCE OF OPERATION:
1. PLANT HOOD VELOCITY CONTROLLER VC-1, RECEIVING AIR FLOW INPUT FROM VELOCITY SENSOR VS-1, SHALL MAINTAIN SETPOINT (ADJUSTABLE) IN VARIABLE SPEED DRIVE VSD-1 TO MAINTAIN SETPOINT (ADJUSTABLE) IN VSD-1.
2. AS AIR FLOW INTO PLANT HOOD IS RESTRICTED BY CLOSING THE HOOD DOORS, PRESSURE CONTROLLER PC-1 SHALL INCREASE DOOR D-1.
3. D-1 WILL PROVIDE FILTER ALARMING WITH PILOT LIGHT.

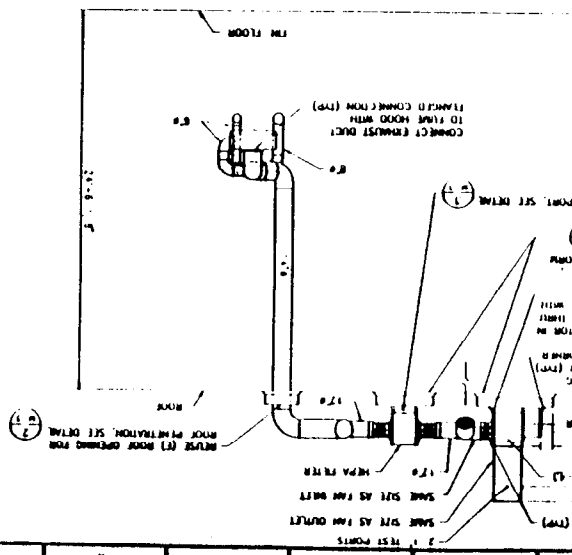
MATERIALS:

ITEM	DESCRIPTION	QTY	UNIT
VC-1	VELOCITY CONTROLLER	1	EA
VS-1	VELOCITY SENSOR	1	EA
VS-2	VELOCITY SENSOR	1	EA
VS-3	VELOCITY SENSOR	1	EA
VS-4	VELOCITY SENSOR	1	EA
VS-5	VELOCITY SENSOR	1	EA
VS-6	VELOCITY SENSOR	1	EA
VS-7	VELOCITY SENSOR	1	EA
VS-8	VELOCITY SENSOR	1	EA
VS-9	VELOCITY SENSOR	1	EA
VS-10	VELOCITY SENSOR	1	EA
VS-11	VELOCITY SENSOR	1	EA
VS-12	VELOCITY SENSOR	1	EA
VS-13	VELOCITY SENSOR	1	EA
VS-14	VELOCITY SENSOR	1	EA
VS-15	VELOCITY SENSOR	1	EA
VS-16	VELOCITY SENSOR	1	EA
VS-17	VELOCITY SENSOR	1	EA
VS-18	VELOCITY SENSOR	1	EA
VS-19	VELOCITY SENSOR	1	EA
VS-20	VELOCITY SENSOR	1	EA
VS-21	VELOCITY SENSOR	1	EA
VS-22	VELOCITY SENSOR	1	EA
VS-23	VELOCITY SENSOR	1	EA
VS-24	VELOCITY SENSOR	1	EA
VS-25	VELOCITY SENSOR	1	EA
VS-26	VELOCITY SENSOR	1	EA
VS-27	VELOCITY SENSOR	1	EA
VS-28	VELOCITY SENSOR	1	EA
VS-29	VELOCITY SENSOR	1	EA
VS-30	VELOCITY SENSOR	1	EA
VS-31	VELOCITY SENSOR	1	EA
VS-32	VELOCITY SENSOR	1	EA
VS-33	VELOCITY SENSOR	1	EA
VS-34	VELOCITY SENSOR	1	EA
VS-35	VELOCITY SENSOR	1	EA
VS-36	VELOCITY SENSOR	1	EA
VS-37	VELOCITY SENSOR	1	EA
VS-38	VELOCITY SENSOR	1	EA
VS-39	VELOCITY SENSOR	1	EA
VS-40	VELOCITY SENSOR	1	EA
VS-41	VELOCITY SENSOR	1	EA
VS-42	VELOCITY SENSOR	1	EA
VS-43	VELOCITY SENSOR	1	EA
VS-44	VELOCITY SENSOR	1	EA
VS-45	VELOCITY SENSOR	1	EA
VS-46	VELOCITY SENSOR	1	EA
VS-47	VELOCITY SENSOR	1	EA
VS-48	VELOCITY SENSOR	1	EA
VS-49	VELOCITY SENSOR	1	EA
VS-50	VELOCITY SENSOR	1	EA
VS-51	VELOCITY SENSOR	1	EA
VS-52	VELOCITY SENSOR	1	EA
VS-53	VELOCITY SENSOR	1	EA
VS-54	VELOCITY SENSOR	1	EA
VS-55	VELOCITY SENSOR	1	EA
VS-56	VELOCITY SENSOR	1	EA
VS-57	VELOCITY SENSOR	1	EA
VS-58	VELOCITY SENSOR	1	EA
VS-59	VELOCITY SENSOR	1	EA
VS-60	VELOCITY SENSOR	1	EA
VS-61	VELOCITY SENSOR	1	EA
VS-62	VELOCITY SENSOR	1	EA
VS-63	VELOCITY SENSOR	1	EA
VS-64	VELOCITY SENSOR	1	EA
VS-65	VELOCITY SENSOR	1	EA
VS-66	VELOCITY SENSOR	1	EA
VS-67	VELOCITY SENSOR	1	EA
VS-68	VELOCITY SENSOR	1	EA
VS-69	VELOCITY SENSOR	1	EA
VS-70	VELOCITY SENSOR	1	EA
VS-71	VELOCITY SENSOR	1	EA
VS-72	VELOCITY SENSOR	1	EA
VS-73	VELOCITY SENSOR	1	EA
VS-74	VELOCITY SENSOR	1	EA
VS-75	VELOCITY SENSOR	1	EA
VS-76	VELOCITY SENSOR	1	EA
VS-77	VELOCITY SENSOR	1	EA
VS-78	VELOCITY SENSOR	1	EA
VS-79	VELOCITY SENSOR	1	EA
VS-80	VELOCITY SENSOR	1	EA
VS-81	VELOCITY SENSOR	1	EA
VS-82	VELOCITY SENSOR	1	EA
VS-83	VELOCITY SENSOR	1	EA
VS-84	VELOCITY SENSOR	1	EA
VS-85	VELOCITY SENSOR	1	EA
VS-86	VELOCITY SENSOR	1	EA
VS-87	VELOCITY SENSOR	1	EA
VS-88	VELOCITY SENSOR	1	EA
VS-89	VELOCITY SENSOR	1	EA
VS-90	VELOCITY SENSOR	1	EA
VS-91	VELOCITY SENSOR	1	EA
VS-92	VELOCITY SENSOR	1	EA
VS-93	VELOCITY SENSOR	1	EA
VS-94	VELOCITY SENSOR	1	EA
VS-95	VELOCITY SENSOR	1	EA
VS-96	VELOCITY SENSOR	1	EA
VS-97	VELOCITY SENSOR	1	EA
VS-98	VELOCITY SENSOR	1	EA
VS-99	VELOCITY SENSOR	1	EA
VS-100	VELOCITY SENSOR	1	EA

MECHANICAL PLAN



A SECTION



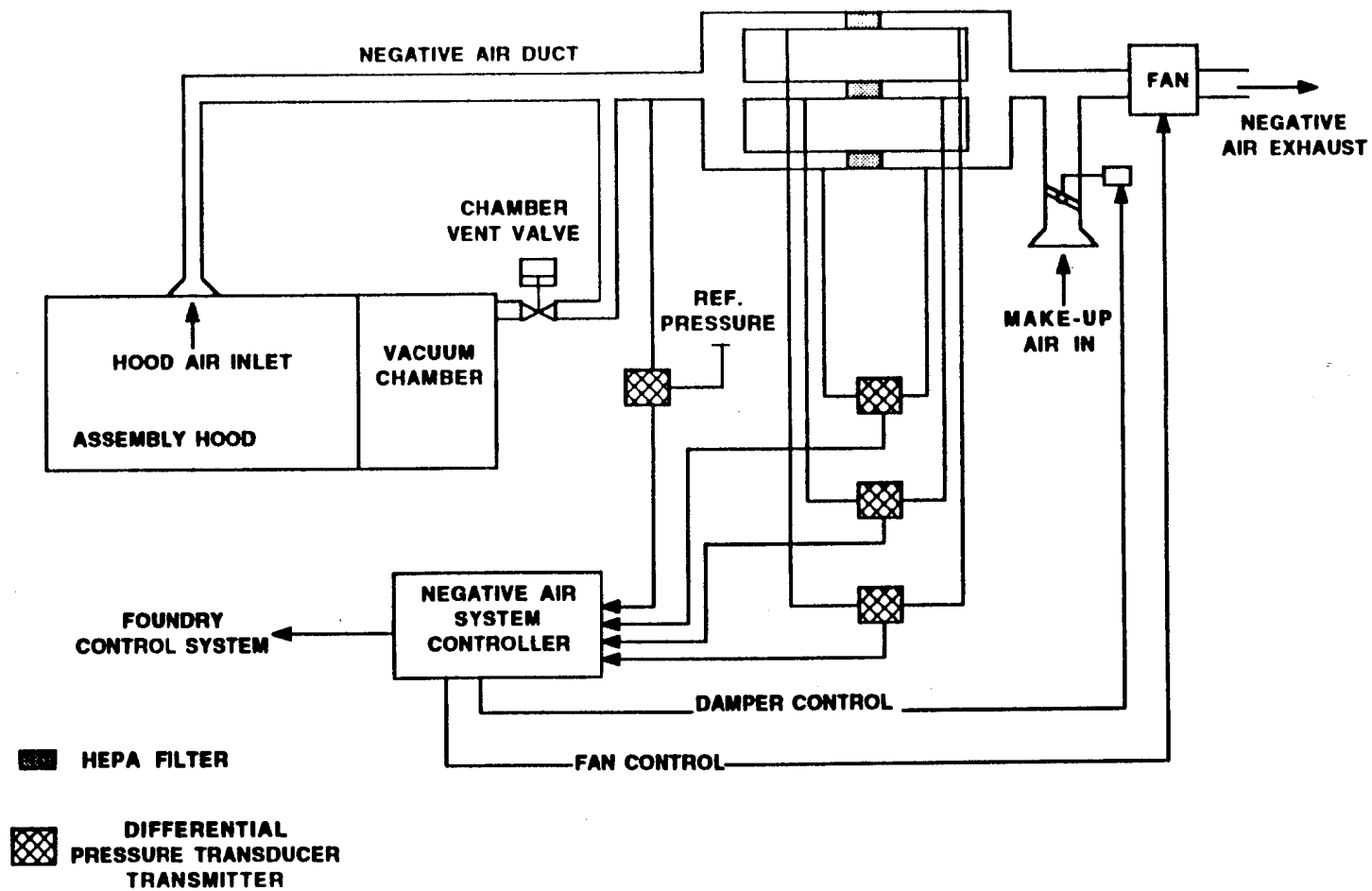
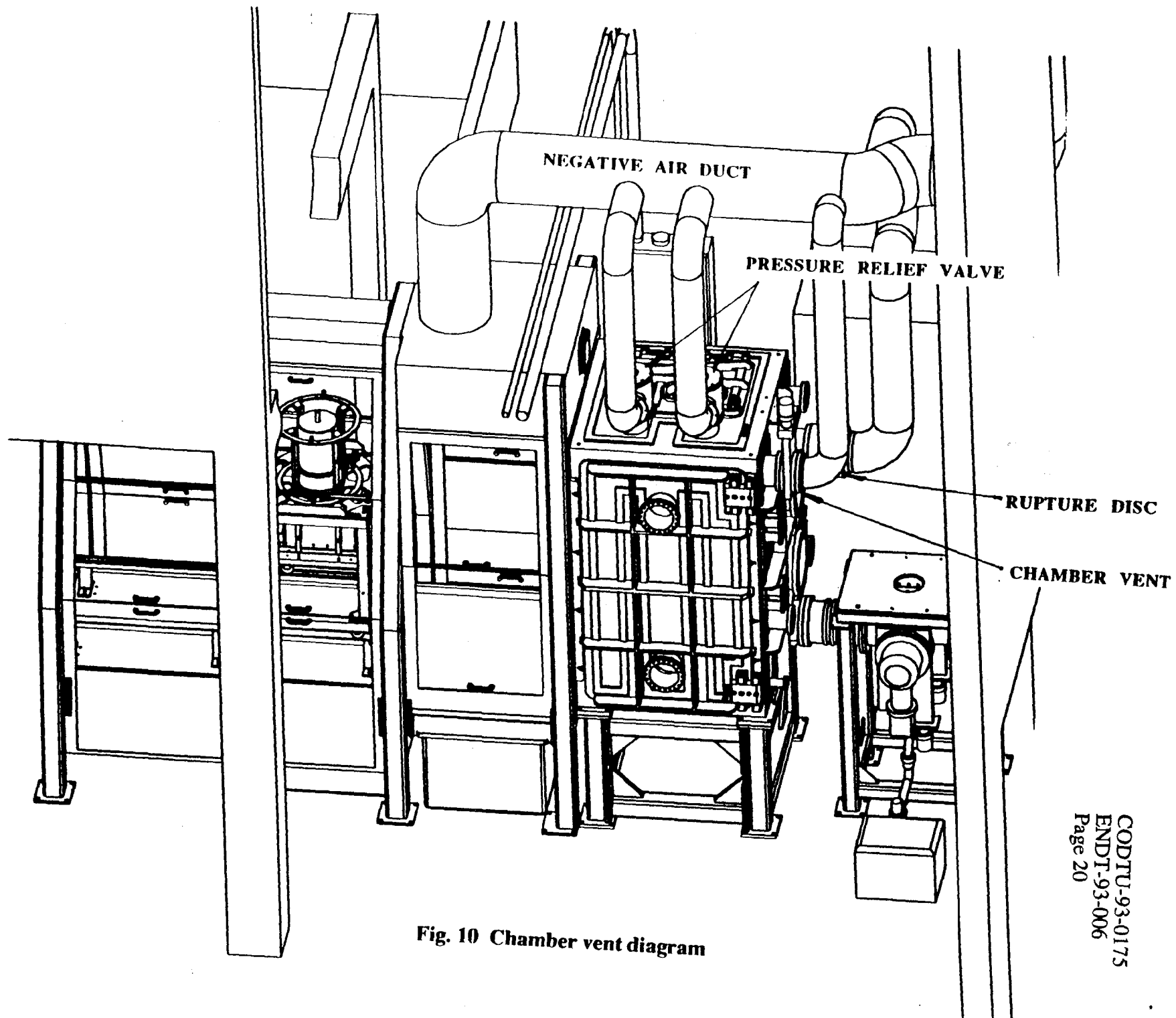


Fig. 9. Schematic of negative air control system

they are assumed to be the leak source in this analysis. The cooling circuits have building back-up power and switch over to city water automatically in the event of a power failure or the closed loop cooling system failure. The city water is drained into a temporary holding tank for sampling of possible contamination prior to returning to the city drain. Each cooling loop has two pressure relief valves to prevent over pressure as described in Section 5.2. The capacity of the closed loop cooling system water tank is 10 gal and the level is monitored to provide an alarm signal to the operator if the level drops below the operating setpoint. The vessel walls are cooled by traced cooling lines welded to the exterior chamber surface. The cooling circuit for these walls is an open loop system and it is independent of the internal closed loop cooling circuit.



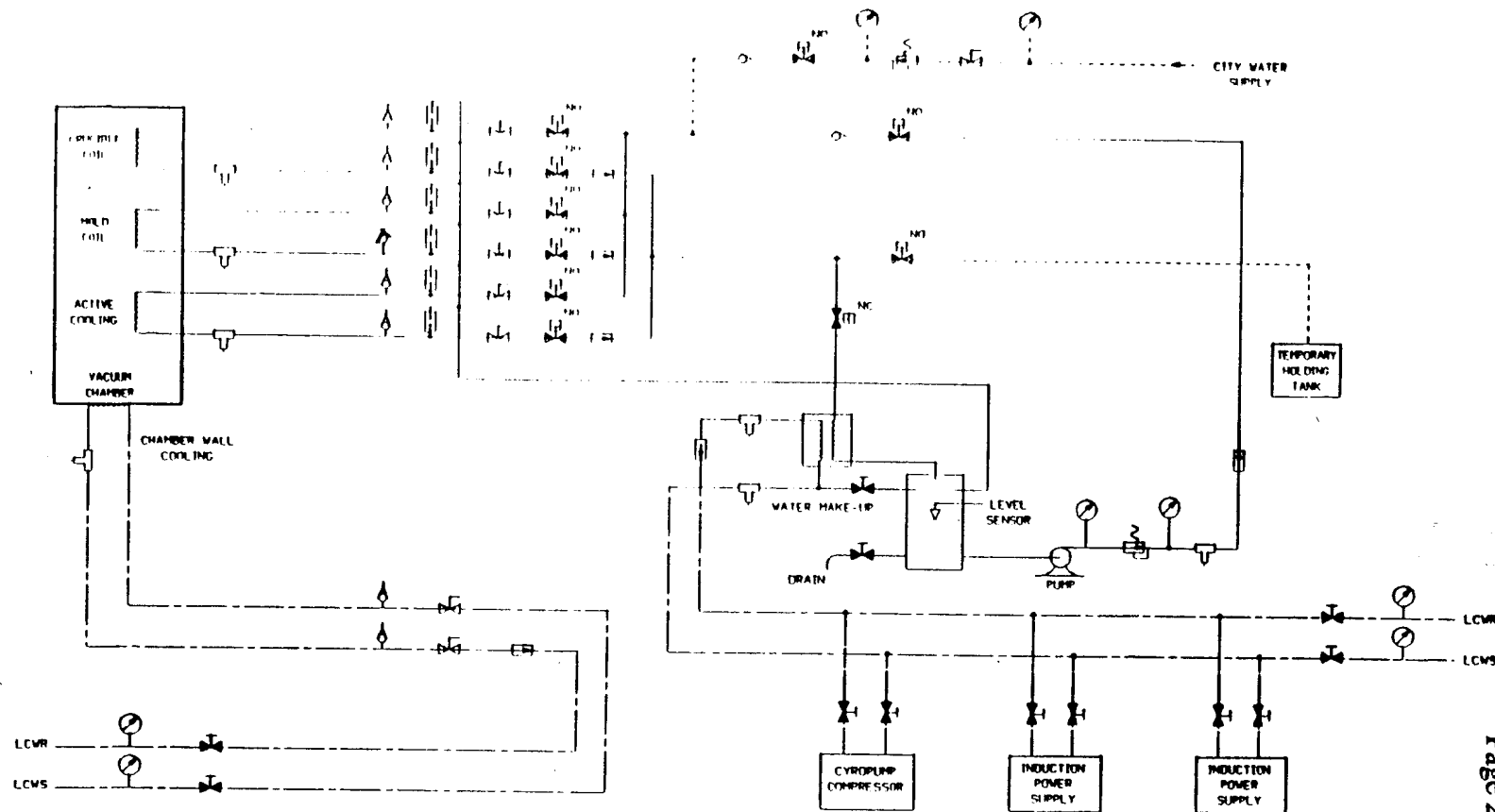


Fig. 11. Uranium foundry water cooling diagram

CODTU-93-0175
ENDT-93-006
Page 21

NO. 1000	PART / U.S. 100	DESCRIPTION / MATERIAL	DATE
1000	1000	VACUUM FURNACE	5/93
1000	1000	URANIUM FOUNDRY	5/93
1000	1000	SCHEMATIC - COOLING SYSTEM	5/93
1000	1000	AAA93-101412-00	5/93
1000	1000	SCALE: 1" = 1'-0"	5/93

THE DESIGN IS THE PROPERTY OF THE UNIVERSITY OF CALIFORNIA (UNIVERSITY OF CALIFORNIA) LABORATORY. REPRODUCTION OF THIS DOCUMENT WITHOUT PERMISSION OF THE UNIVERSITY OF CALIFORNIA IS PROHIBITED.

LAWRENCE LIVERMORE NATIONAL LABORATORY UNIVERSITY OF CALIFORNIA

7.0 Reference

1. Memo C.S. Landram to J. Sze, "Closure on Fauske & Associates, Inc., Safety Analysis for the Uranium Vacuum Induction Furnace," TFG93-037, June 29, 1993.
2. "Safety Analysis of Furnace Assembly in the Uranium Foundry," Mechanical Engineering Safety Note, ENDT-93-902.
3. Mechanical Engineering Design Safety Standards, M-012 Rev. 6, Section 3.1 - Pressure Vessels and Systems, 1982.
4. "Work Enclosures for Toxic and Radioactive Materials," LLNL Health & Safety Manual, Supplement 12.03, August 1991.

Appendix A

Safety analysis for the Uranium Vacuum Furnace

FAI/93-35

**SAFETY ANALYSIS FOR
THE URANIUM VACUUM
INDUCTION FURNACE**

Submitted To:

**Lawrence Livermore National Laboratory
Post Office Box 808
Livermore, California 94550**

Prepared By:

**Fauske & Associates, Inc.
16W070 West 83rd Street
Burr Ridge, Illinois 60521**

June, 1993

TABLE OF CONTENTS

	<u>Page</u>
1.0 INTRODUCTION	1-1
2.0 ACCIDENT CONDITIONS ANALYZED	2-1
2.1 Description of the Design Analyzed	2-1
2.2 Postulated Accident States for the Safety Analysis	2-10
3.0 UPDATE OF BASIC CONSIDERATIONS FOR STEAM EXPLOSIONS AND HYDROGEN BURNS	3-1
3.1 Steam Explosions	3-1
3.1.1 FAI Thermite Experiments	3-2
3.1.2 Sandia FITSB Tests	3-5
3.1.3 Summary	3-12
3.1.4 Possible Mechanism for Maximum Steam Generation Rate	3-13
3.1.5 Shock Waves from Steam Explosions	3-15
3.1.6 Metal-Water Reactions During Explosive Interactions	3-18
3.2 Hydrogen Burns	3-18
4.0 STEAM EXPLOSION EVALUATION	4-1
5.0 HYDROGEN BURN EVALUATION	5-1
6.0 RELIEF REQUIREMENTS	6-1
7.0 OPERATIONAL CONSIDERATIONS	7-1
8.0 MELT-THROUGH	8-1
9.0 SUMMARY AND CONCLUSIONS	9-1
10.0 REFERENCES	10-1

LIST OF FIGURES

<u>Figure No.</u>		<u>Page</u>
2-1	Proposed apparatus	2-2
2-2	Overall system dimensions	2-3
2-3	Proposed furnace enclosure	2-4
2-4	Melting crucible for the uranium metal	2-5
2-5	Position of the crucible	2-6
2-6	Relative location of the melt crucible and mold	2-7
3-1	Measured debris-water energy transfer rates from EPRI sponsored Mark I liner tests	3-3
3-2	FITS containment chamber	3-6
3-3	FITS2B chamber air pressure	3-9
3-4	FITS3B chamber air pressure	3-10
3-5	FITS6B chamber air pressure (saturated water)	3-11
3-6	Debris dispersion configuration	3-14
3-7	Comparison of shock wave pressures for TNT and point source explosions	3-16
3-8	Normalized peak pressure (P_{max}/P_0) for hydrogen: air:diluent mixtures, comparing CO_2 and steam (AICC - adiabatic isochoric complete combustion, Rh = relative humidity) (Benedick, 1984)	3-20
3-9	Hydrogen:air:steam flammability data with fans off (Marshall, 1986)	3-21
3-10	Hydrogen:air:steam flammability data with fans operational (Marshall, 1986)	3-22
3-11	Hydrogen:air:steam flammability data with fans on and off shown with the exponential curve fit (Marshall, 1986)	3-24

LIST OF TABLES

<u>Table No.</u>		<u>Page</u>
2-1	Parameter List for Induction Vacuum Furnace	2-8
3-1	Effective Heat Flux Measurements for Debris-Water Interactions	3-4
3-2	FITSB Initial Conditions and Observations	3-7
3-3	Chamber Air Pressure Data from FITSB (Times from Melt Entry)	3-17

1.0 INTRODUCTION

The proposed design for the induction vacuum furnace would provide for 100 Kg of molten uranium metal in the induction heated crucible and subsequently drain into the mold beneath the crucible. The design includes three water cooling systems, one for the crucible induction heating coil, the second for the mold induction heating coil and the third for the active cooling in the mold. Since these coils could develop leaks either due to extended use, or as the result of an accident condition, the potential for a melt-water thermal interaction (steam explosion) and the possibility of hydrogen created by steam oxidation of the molten uranium must be considered in the safety analysis. This report describes the design of the furnace used for this evaluation, the postulated accident states considered in the analysis, the basic considerations associated with steam explosions and hydrogen burns, individual evaluations for steam explosions, hydrogen burns and relief requirements, operational considerations which would enhance the safety philosophy, and the potential for melt-through of the molten uranium metal should it spill onto the furnace floor.

2.0 ACCIDENT CONDITIONS ANALYZED

2.1 Description of the Design Analyzed

Figures 2-1, 2-2 and 2-3 illustrate the vacuum furnace investigated with respect to the potential for molten uranium-water interactions. Table 2-1 lists the pertinent parameters for the vacuum chamber, the crucible assembly, the mold assembly, the catch basin and the cooling coils. Figure 2-4 shows the crucible used to melt the uranium by induction heating. By withdrawing the stopper rod, the melt drains into the mold below. Figures 2-5 and 2-6 show the orientation of the crucible and the mold assembly.

In these analyses, there are two locations where water and melt could be potentially accumulated during an accident where they may come into intimate contact. The first is the mold assembly and the second is the floor of the vacuum furnace. As described in Table 2-1 the inside diameter of the mold is 16 in. (40.6 cm) which corresponds to an area of 1.40 ft² (0.13 m²) and the floor of the vacuum furnace which is 36 in. by 36 in. (91.4 cm by 91.4 cm) or an area of 9 ft² (0.84 m²). These two locations represent the two primary regions where either melt or water could be collected and come into intimate contact. This will be discussed in the following sections.

Item No. 5 of Table 2-1 describes the volume of water available in the crucible induction coil, the mold induction coil and the active cooling for the mold. Typically, only one of these systems would be anticipated to fail, but in the following section an end-of-spectrum accident condition will be considered in which all of the water coils will be assumed to be broken with the water inventory spilled onto the floor of the vacuum chamber. The safety philosophy for the furnace is to isolate the coolant flow where any accident condition is detected, which is principally indicated by a loss of vacuum. Considering the response time to shut off the cooling water, the maximum amount of water available for reaction inside the chamber will conservatively be taken to be 10 gal. (Information provided from John S. Sze to Hans K. Fauske, letter dated June 1, 1993.)

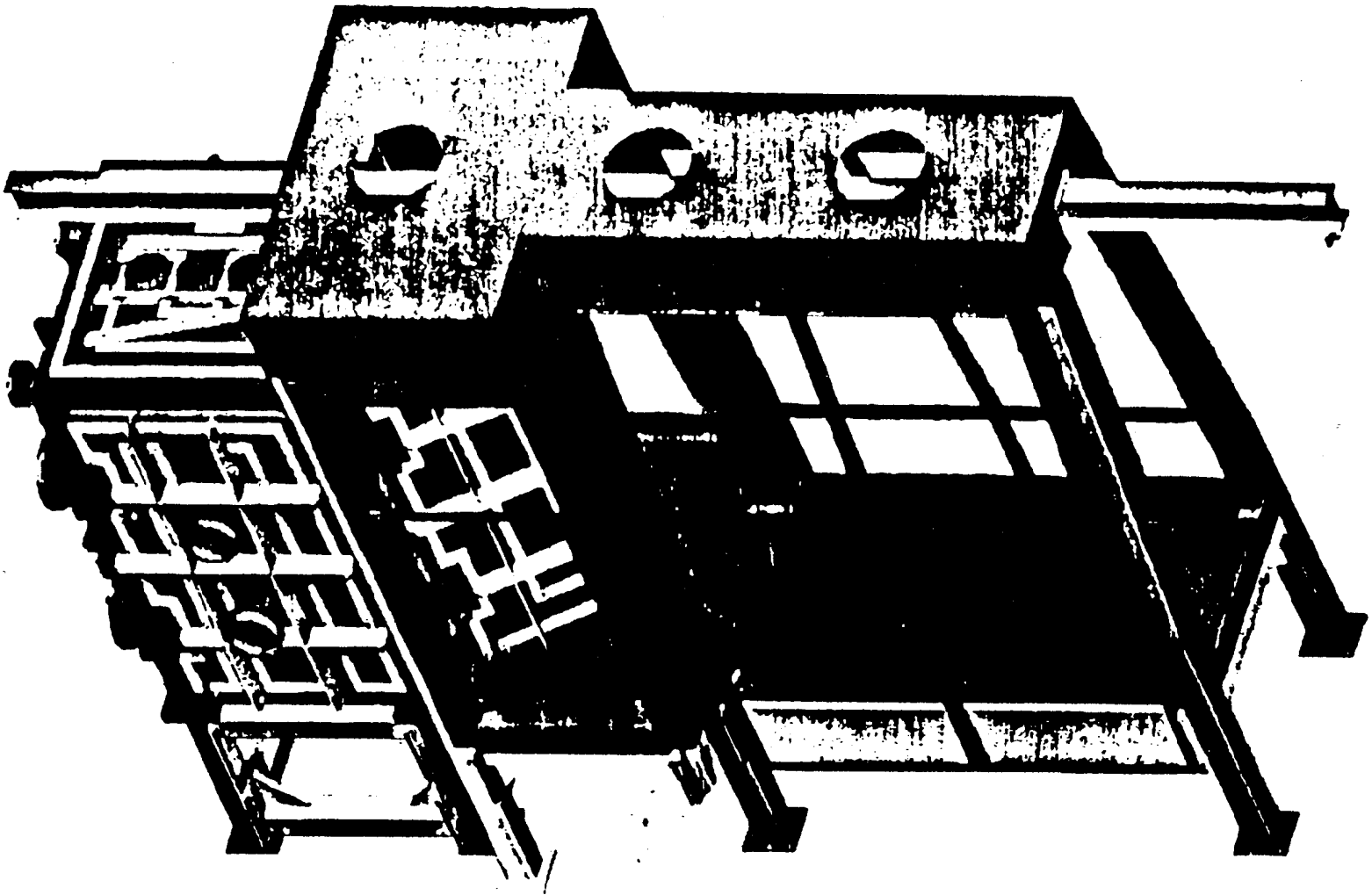
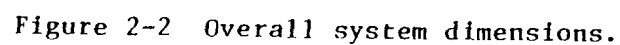


Figure 2-1 Proposed apparatus.



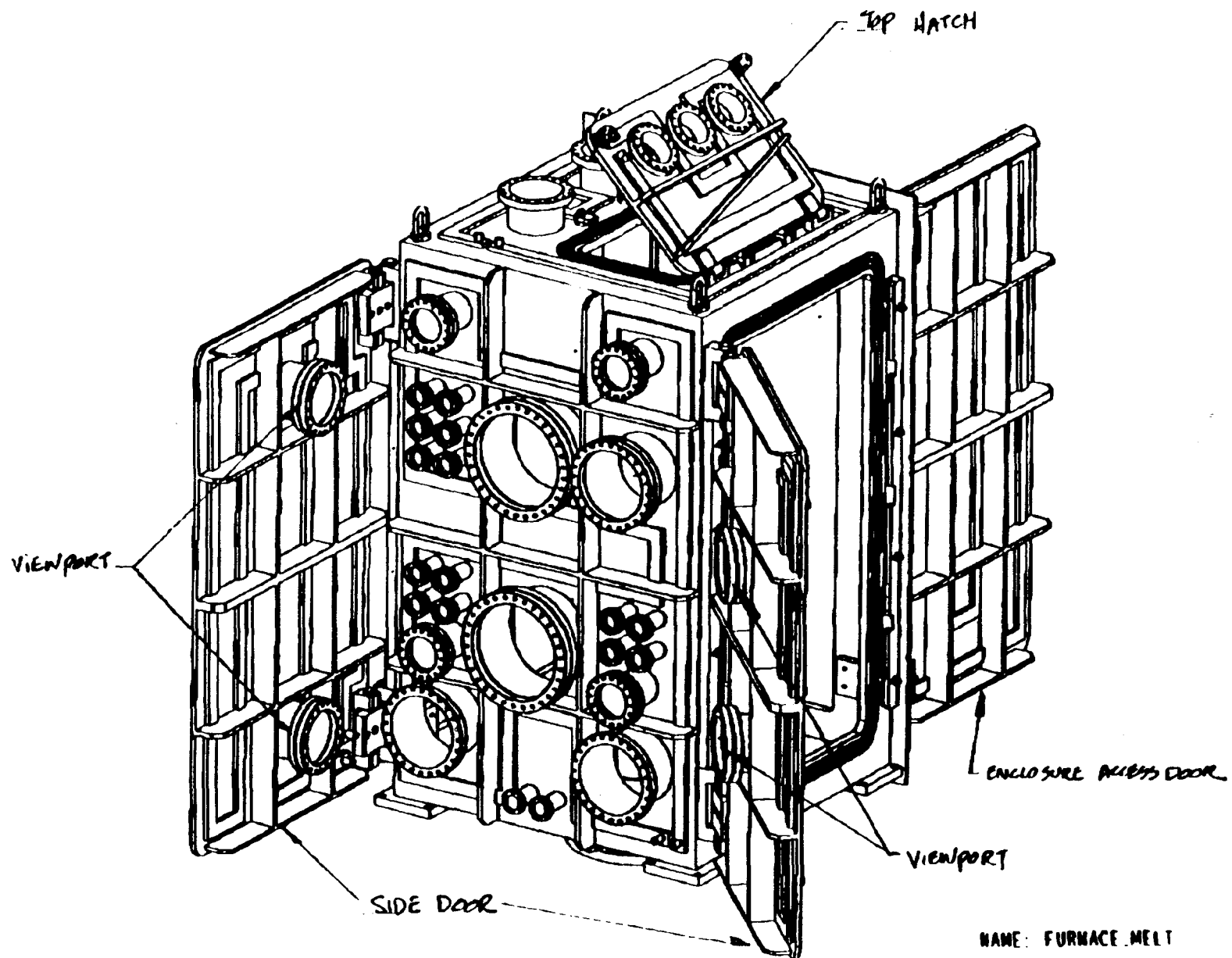
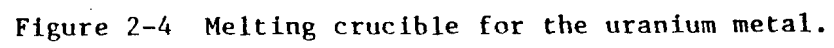
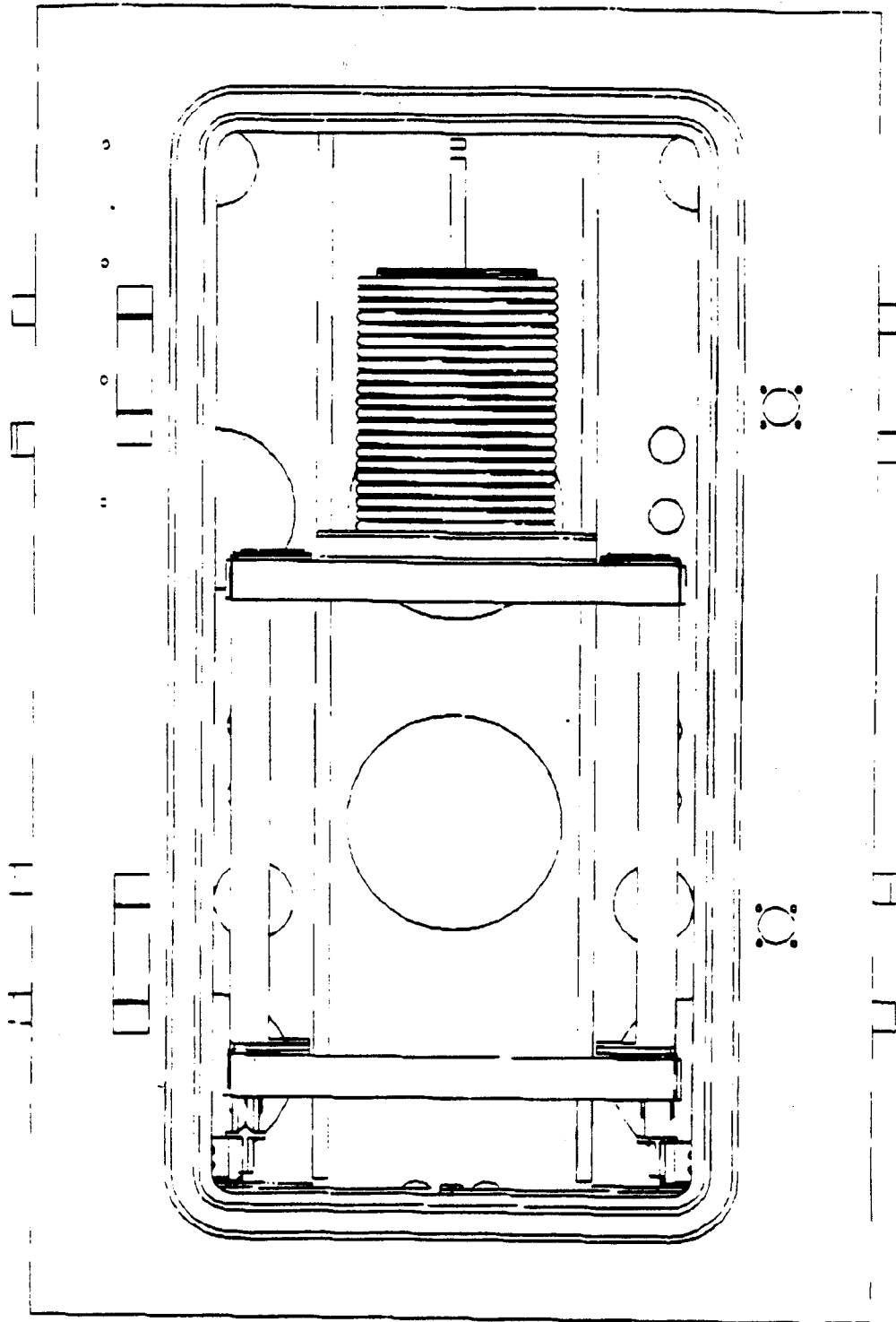


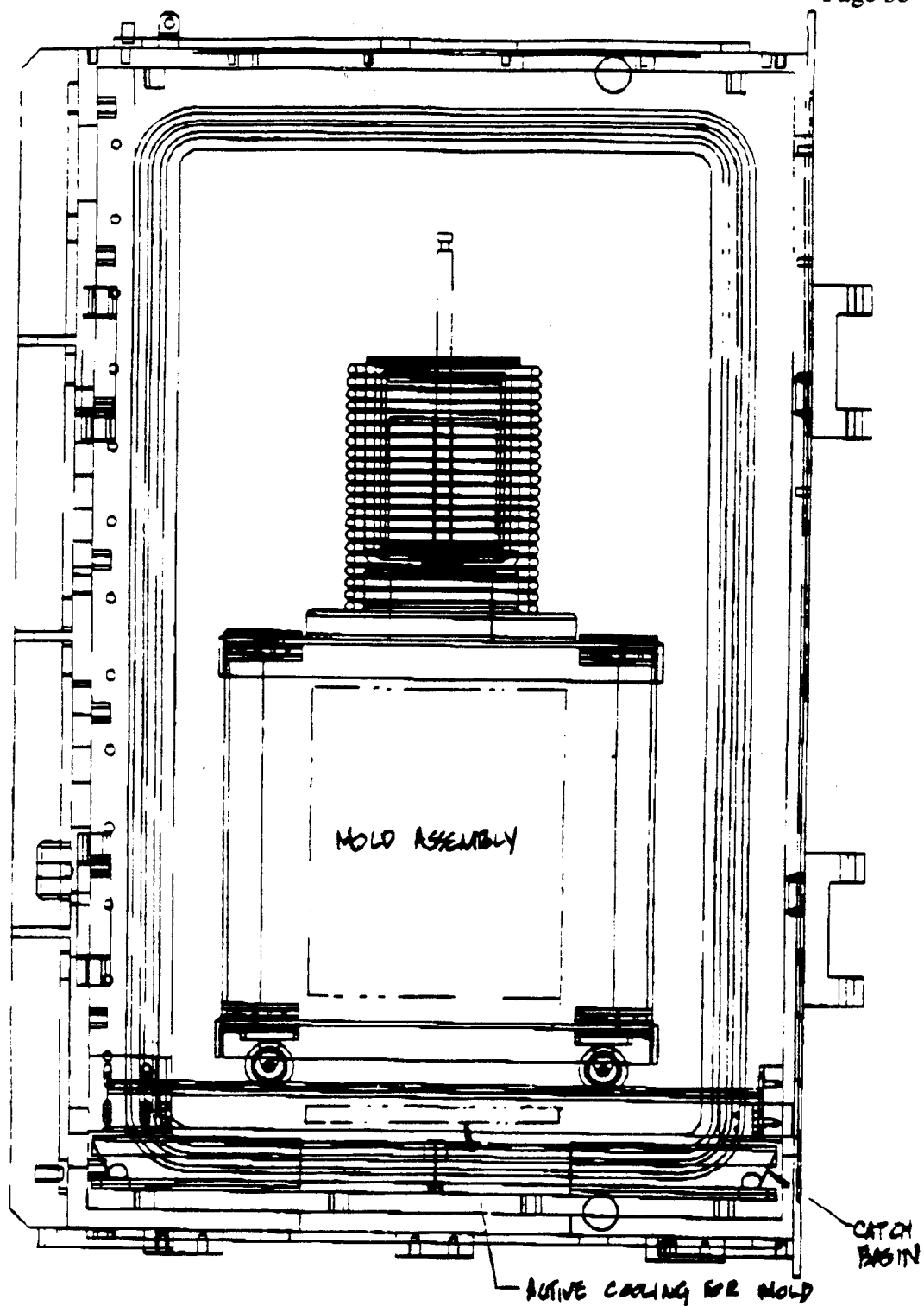
Figure 2-3 Proposed furnace enclosure.





LOOKING IN FROM THE ENCLOSURE ACCESS DOOR

Figure 2-5 Position of the crucible.



LOOKING IN FROM THE SIDE DOOR

Figure 2-6 Relative location of the melt crucible and mold.

Table 2-1

PARAMETER LIST FOR INDUCTION VACUUM FURNACE

1. Vacuum Chamber

- | | |
|---|--|
| • Chamber Size and Material:
Vacuum Vessel | Refer to drawings for detail.
38" x 38" x 62" H (Outside)
36" x 36" x 60" H (Inside)
1.00" THK. 304 Stainless Steel |
| Two Side Doors* (51.5" x 27.5") | .625" THK. 304 Stainless Steel |
| Top Hatch* (21.5" x 13.5") | .500" THK. 304 Stainless Steel |
| Enclosure Access Door*
(53.5" x 24") | .625" THK. 304 Stainless Steel |
| • Operating Pressure | $< 10^{-5}$ Torr. |
| • Support Structure Material | 4" x 4" x .25" Wall Steel Tubing |
| • Four Vacuum Viewports | 6" dia., Located on Both Side Doors |

2. Crucible Assembly

- | | |
|-------------------------|-------------------------------|
| • Crucible Size | See attached crucible layout. |
| • Material | Mullite (Al_2O_3) |
| • Crucible Lid Material | Mullite (Al_2O_3) |
| • Stopper Rod | 0.75" Dia. x 15" L (Mullite) |
| • Uranium Charge (D-38) | 100 Kg Maximum |
| • Operating Temperature | Approx. 1500°C |
| • Induction Coil | Oxygen-Free Copper Tubing |
| • Input Power | 100 kW maximum |

*Double O-ring sealed door.

Table 2-1

PARAMETER LIST FOR INDUCTION VACUUM FURNACE
 (Continued)

3. Mold Assembly

• Mold Material	Tantalum
• Weight of Mold Materials	Approx. 100 Kg
• Mold Size	Approx. 16" Dia. x 20" L
• Operating Temperature	800°C-1200°C
Induction Coil	Oxygen-Free Copper Tubing 20" I.D. x 22" Coil Length
• Input Power	150 kW Maximum

4. Catch Basin*

• Material	0.02 THK. Tantalum Sheet
• Size	3' x 3'

5. Water Available for Thermal Reaction

- The coolant rates of flow are estimated as follows:

Crucible Induction Coil	2.5 GPM
Mold Induction Coil	9.5 GPM
Active Cooling for Mold	3.0 GPM

- Volume of water (internal coils and the length to control valves):

Crucible Induction Coil	80 in ³
Mold Induction Coil	206 in ³
Active Cooling for Mold	80 in ³

*For the sake of the safety analysis, the water accumulated is to be assumed available to contact molten uranium. However, the catch basin is designed to permit as much as 4 gal. to drain without puddling in catch basin.

2.2 Postulated Accident States for the Safety Analysis

Several ways are considered in which molten uranium and water could come into contact. These include:

- rupture of the mullite crucible holding the molten uranium resulting in the melt contacting the water cooled copper induction coil,
- accumulation of water in the mold due to a failure of one or more of the cooling coils and a subsequent release of melt into the mold, and
- accumulation of water on the floor of the furnace and a subsequent release of molten uranium onto the floor of the furnace.

These are ordered in their likelihood of occurrence. While none of these are considered to be frequent occurrences, the potential for a small leak in the mullite crucible which might result in direct contact of molten uranium on the induction coils, is far more likely than a large rupture of coolant lines that could accumulate in either the mold or the bottom of the furnace. However, the rupture of the mullite crucible and leakage of uranium onto the water cooled copper tubing used for the induction coil should not result in the failure of the induction coil. The first consideration is the temperature of the coil that would occur if molten uranium, at 1500°C, were to come into direct contact with the copper coil. The temperature upon contact between the uranium and the copper coil is given by

$$T_1 = \frac{T_U + T_C \sqrt{\frac{k\rho c)_c}{k\rho c)_U}}{1 + \sqrt{\frac{k\rho c)_c}{k\rho c)_U}} \quad (2-1)$$

where T_U and T_C are the respective temperatures of the uranium and copper with k , ρ and c representing a thermal conductivity, density and specific heat of the copper (subscript c) and uranium (subscript U). Using typical

values for the properties of uranium metal and copper, the contact temperature between the two materials if the mullite crucible were to rupture is about 400°C. This is well below the temperature required to freeze the uranium and also well below the copper melting temperature. As a result, it would be expected that the uranium would begin to freeze and form a crust around the failure location and the copper would not be melted.

Equation (2-1) only describes the interface temperature before the thermal wave penetrates the wall. After this interval the response of the wall is determined by the boundary condition on the coolant (water) side of the tube and the response of the uranium crust formed during the thermal penetration.

Following the inception of crust formation, the thermal penetration of the copper tube wall would be much less than 1 sec. and would be followed by nucleate boiling on the inner surface of the copper tube. The heat flux to, and through, the copper tube would then be limited by conduction through the uranium metal crust. Considering this to be given by conduction through the crust with an interface temperature equal to the 400°C value calculated above, this results in a heat flux through the copper tubing which is $\sim 6 \text{ MW/m}^2$ after 1 sec. This is in the range of the critical heat flux for highly subcooled water (Tong, 1965). Consequently, it is anticipated that this rapid transient would not result in any significant potential for dryout on the inner surface of the copper coil and, hence, would not result in any damage to the induction coil.* With the continual flow of water through the cooling coil, it is expected that the energy transfer on the inner side of the copper would be removed by nucleate boiling sufficient that the copper wall would not overheat and that the flux through the copper wall would be determined by the thickness of the uranium crust frozen on the copper surface. As a result, the uranium crust

*It is noted here that one cannot apply a steady-state boiling curve to assess whether dryout would be induced within an interval comparable to bubble growth and departure times, i.e. the order of 0.1 sec. For this assessment we have used 1 sec. as the end of the transient period.

would continue to grow and the interface temperature would decrease due to sustained nucleate boiling of the water inside the copper tube.

This leaves two other conditions that need to be evaluated, i.e. accumulation of material within the mold and the accumulation of material on the furnace floor. Accident conditions considered for these two configurations are that one or more coolant lines could be broken due to an external event, such as shaking by a seismic event, with water accumulating in either the mold or the furnace floor. Subsequent to this, the plug could perhaps be also broken or lifted out with melt pouring into the mold. This could cause interaction with the water assumed to be in the mold.

A second consideration would be for the molten uranium to drain onto the furnace floor as a result of the accident condition. Along with these conditions, it is assumed that the vacuum could be broken and air could enter into the furnace. As part of this, the water lines would be isolated and thereby limit the water mass to about 10 gallons. According to the coolant flow rates for the three coils listed in Table 2-1, the accumulation of 10 gallons of water allows about 40 secs. to shut off the supply of water.

3.0 UPDATE OF BASIC CONSIDERATIONS FOR STEAM EXPLOSIONS AND HYDROGEN BURNS

3.1 Steam Explosions

In 1990, two evaluations were performed for the safety assessment of the UDS process vessel; the first evaluated the consequences of steam explosions (FAI, 1990a) and the second considered the influence of hydrogen generation and combustion (FAI, 1990b). The steam explosion evaluation for the UDS vessel included an extensive discussion with respect to basic considerations of vapor explosions including:

- vapor explosion criteria,
- premixing,
- propagation and fine scale mixing, and
- vapor explosion damage potential.

In January of 1993, a CSNI Specialist Meeting on Fuel-Coolant Interactions (steam explosions) was hosted by the University of California at Santa Barbara with the individual papers addressing one or more of these various topics. In summary, the only potential change to the evaluation provided in 1990 is that detailed computer codes (Fletcher and Denham, 1993; Angelini, et al., 1993) have been developed to evaluate the potential for premixing. These have provided more robust evaluations of the fundamental limitations with respect to premixing. Specifically, these detailed calculations show a rapid depletion of water in the mixing zone as a result of heat transfer from the melt to the water during the premixing stage resulting in hydrodynamic limitations with respect to water remaining in this region. Hence, the only specific update necessary to the 1990 analytical considerations are those related to premixing which further, and more eloquently, evaluate the potential limitations for premixing of a high temperature molten metal and water to initiate an explosive interaction. However, there have been additional experimental results made available that, with interpretation, are useful in these safety evaluations.

3.1.1 FAI Thermite Experiments

Two sets of experiments have been performed at FAI in which 44 lbm (20 kg) of molten iron-thermite was injected into water. The first (Malinovic, et al., 1989) was performed to study the role of water in protecting the Mark I containment liner under severe accident conditions and is discussed extensively in the steam explosion evaluation for the UDS process vessel (FAI, 1990a). The second (Henry, et al., 1991) addressed the influence of water during a high pressure melt ejection. Both of these represent conditions which could cause ex-vessel steam explosions and both facilities were instrumented sufficiently to estimate the steam generation rates resulting from these interactions.

Interpretation of the rate, in terms of a heat flux based upon the projected floor area where the interaction occurs, provide a means of applying the results to another system. Figure 3-1 illustrates the measured heat flux to the overlying water pool in the Mark I experiments when the test apparatus was instrumented to detect the energy transfer to the test box walls. All tests show a very high energy transfer rate within the first few seconds, the value being between 6.3×10^6 and 9.5×10^6 Btu/h-ft² (20 and 30 MW/m²), which subsequently decreased to about 0.28×10^6 Btu/h-ft² (0.9 MW/m²) after the debris is frozen. In this set of experiments, 11 tests were performed, 10 of which had water available in the simulated containment prior to the discharge of the molten iron thermite. In all 10 experiments, rapid energy transfer rates (6.3×10^6 - 9.5×10^6 Btu/h-ft² (20-30 MW/m²)) were observed when the debris was discharged into the water.

FAI direct containment heating experiments (Henry, et al., 1991) also had sufficient instrumentation to estimate the steam generation rates when debris was discharged from the simulated RCS into the reactor cavity and subsequently up onto the containment floor. Table 3-1 summarizes the information for these experiments in terms of the energy transfer rate in the cavity for the three experiments in which water was available (DCH-1, DCH-2, and DCH-4) and also for the energy transfer rates from the debris to the water as the debris was discharged onto the containment floor. Values

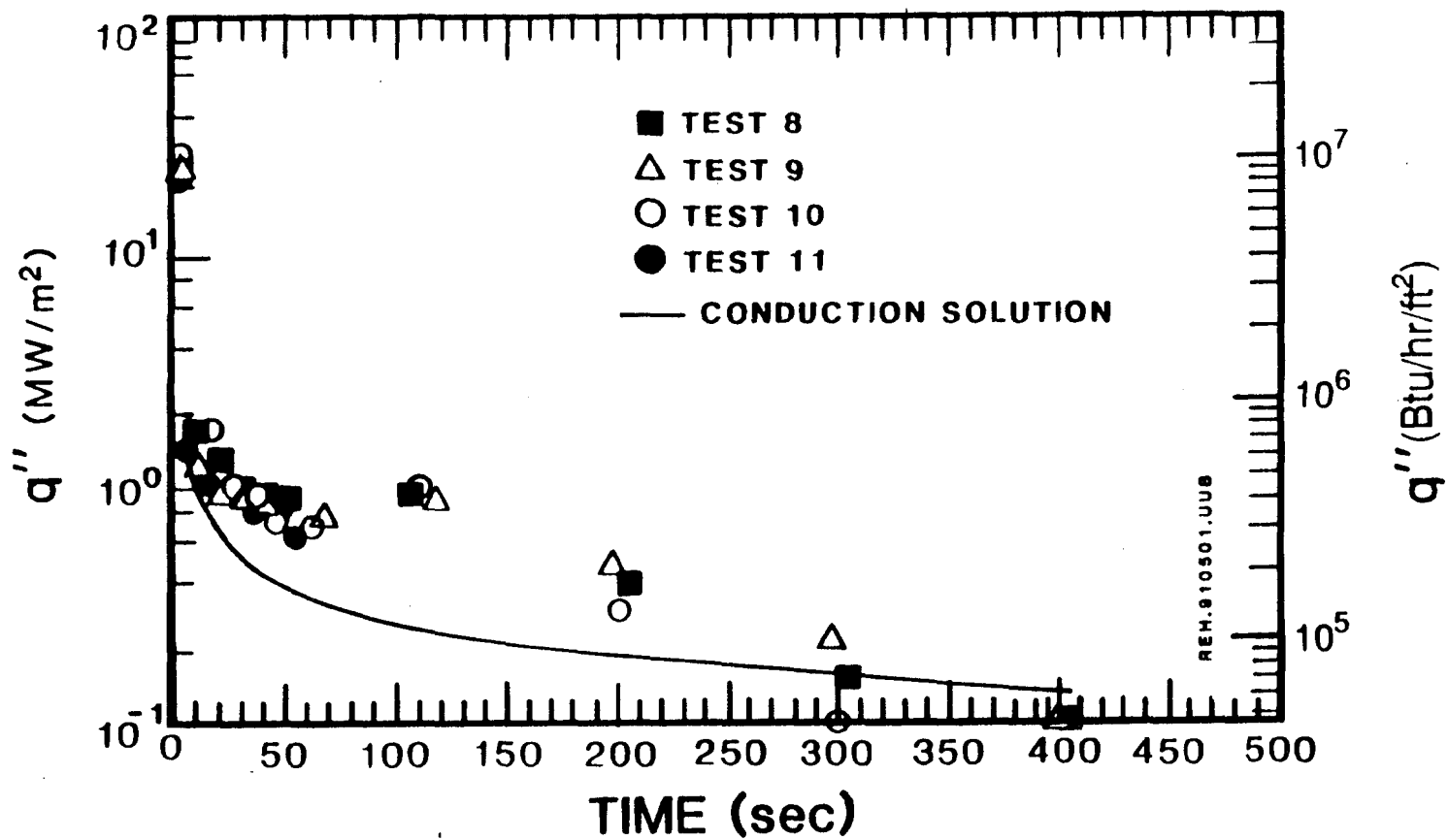


Figure 3-1 Measured debris-water energy transfer rates from EPRI sponsored Mark I liner tests.

Table 3-1

EFFECTIVE HEAT FLUX MEASUREMENTS FOR DEBRIS-WATER INTERACTIONS

Test	<u>Initial Pressurization</u>		<u>Intermediate Period</u>		<u>Long Term Quenching</u>	
	M Btu/h-ft ²	MW/m ²	M Btu/h-ft ²	MW/m ²	M Btu/h-ft ²	MW/m ²
DCH-1	4.75/13.3°	15/42°	3.49/6.02°	11/19°	2.75/5.5°	8.5/17.5°
DCH-2	2.22/10.78°	7/34°	4.12/6.66°	13/21°	2.31/5.17°	7.3/16.3°
DCH-3	N/A	N/A	N/A	N/A	1.27/4.12°	4/13°
DCH-4	1.27/9.83°	4/31°	3.49/6.02°	11/19°	N/A/2.85°	N/A/9°

*Contribution from the heat sinks added to the vaporization calculation.

are also given for estimated additional energy transfer due to the transfer into the steel structural heat sinks in the simulated containment lower compartment. These additional energy transfer rates should be summed with those determined from the containment compartment pressurization rates. As illustrated by this table, the energy transfer rates are large and comparable to those observed in the Mark I tests. These rates are an order of magnitude greater than those typical of the critical heat flux (CHF) for a horizontal upward facing surface.

3.1.2 Sandia FITSB Tests

Later Sandia FITS tests have provided sufficient pressure transient information to evaluate the average steam generation rate resulting from explosive interactions. Steam generation rates can then be divided by the cross-sectional area of the FITS vessel to determine the effective heat fluxes. Figure 3-2 taken from (Mitchell, et al., 1986) shows a cross-section of the FITS facility. In this test series, about 18.6 kg (41 lbm) of molten thermite was poured into water test containers located in the FITS chamber and the resultant pressure history in the chamber gas space was recorded. Table 3-2, which was also taken from (Mitchell, et al., 1986), summarizes the test conditions and observations made with respect to explosive interactions. Figures 3-3 through 3-5 illustrate the pressurization of the gas space, the first two with initially subcooled water and the last with saturated water.

While only some of the experiments had explosive interactions, the principal focus is on the net steam generation rate created by the explosive interaction. The large steel vessel is considered to be pressurized with steam with the realization that this also increases the potential for condensation on the vessel walls. The results shown in Figures 3-3 through 3-5 are those with the largest vessel pressurization. A comparison of these figures also shows that the time to the peak pressure is ~ 1 sec. for these tests, even though the path to this pressure may differ somewhat. (Test FITS 7B experienced about 90% of the pressure increase in the first second with the remainder occurring over the next 3 secs.)

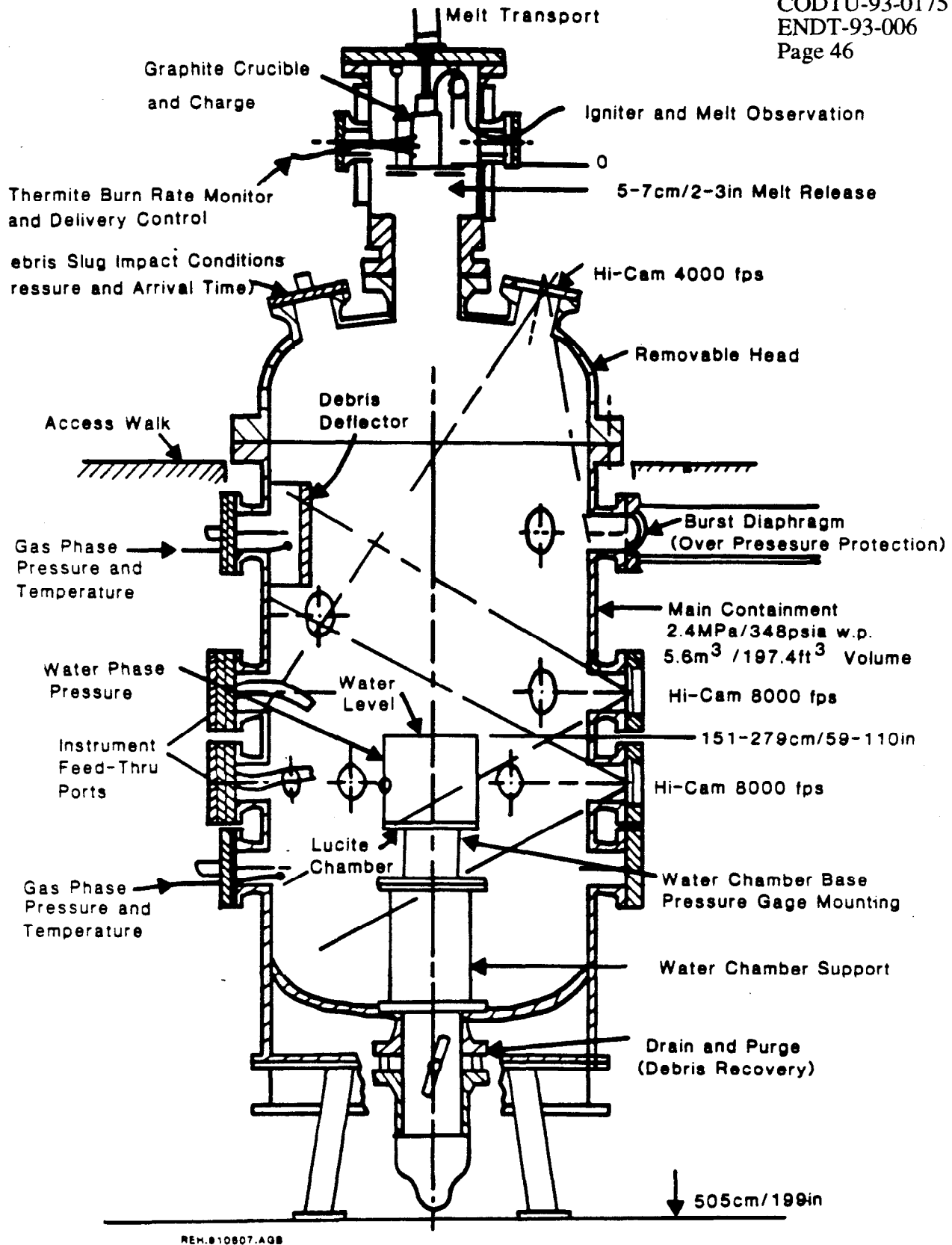


Figure 3-2 FITS containment chamber.

Table 3-2

FITSB INITIAL CONDITIONS AND OBSERVATIONS

Expt	Melt			Water			Initial Ratio Water/Melt		Spontaneous Explosion		Other Observations
	Mass (kg)	Entry Vel (m/s)	Avg Dia at Entry ¹ (cm)	Geometry (cm) Sq x Deep	Mass (kg)	Temp (K)	Mass	Vol ²	Location	Time After Melt Entry (ms)	
1B	18.7	5.4	4.1	61 x 61	226.0	298	12.0	46.0	Surface Unknown	142 275	First explosion Second explosion
2B	18.6	6.0	6.0	61 x 30	113.0	298	6.0	23.0	Surface	84	Single explosion
3B	18.6	6.0	24.0	43 x 30	57.0	295	1.0	11.5	Base	77	Single explosion weak interaction at surface at 70 ms after entry that did not propagate
4B	18.7	6.8	5.8	61 x 61	226.0	299	12.0	46.0	Surface Base	29 146	First explosion Second explosion
6B	18.7	7.2	6.5	46 x 30	63.4	367	3.4	12.9	None	-	Multiple interactions at 40, 57, 82 and 153 ms after melt entry, no propagation of steam explosion.
7B	18.7	7.4	n.o. ³	43 x 15.2	28.1	291	1.5	5.7	n.o.	80	No camera data, time estimated from water phase gauges.
8B	18.7	6.5	29.0	61 x 76.5	283.5	288	15.0	57.4	Surface Base	27 146	First explosion Second explosion
9B	18.7	7.0	5.8	61 x 45.7	170.0	289	9.0	34.6	Base	98	Single explosion

¹Optical measurement.²Melt density 3.8 g/cm³.³Not observed.

Table 3-2
(Continued)

FITSB INITIAL CONDITIONS AND OBSERVATIONS
(English Units)

Expt	Melt			Water			Initial Ratio Water/Melt		Spontaneous Explosion	
	Mass (lbm)	Entry Vel. (ft/s)	Avg Dia at Entry ¹ (in)	Geometry (in) Sq x Deep	Mass (lbm)	Temp (°F)	Mass	Vol ²	Location	Time After Melt Ent (ms)
1B	41.2	17.71	1.61	24 x 24	498.0	77	12.0	46.0	Surface Unknown	142 275
2B	41.0	19.68	2.36	24 x 11.8	249.0	77	6.0	21.0	Surface	84
3B	41.0	19.68	9.45	17 x 11.8	125.7	71.6	3.0	11.5	Base	77
4B	41.2	22.31	2.28	24 x 24	498.0	78.8	12.0	46.0	Surface Base	29 146
6B	41.2	23.62	2.56	18 x 11.8	139.8	201.2	3.4	12.9	None	
7B	41.2	24.28	n.o. ³	17 x 6	61.95	64.4	1.5	5.7	n.o.	80
8B	41.2	21.33	11.42	24 x 30	625.0	59.0	15.0	57.4	Surface Base	27 146
9B	41.2	22.97	2.2	24 x 18	374.79	60.8	9.0	34.6	Base	98

¹Optical measurement.

²Melt density 3.8 g/cm³

³Not observed

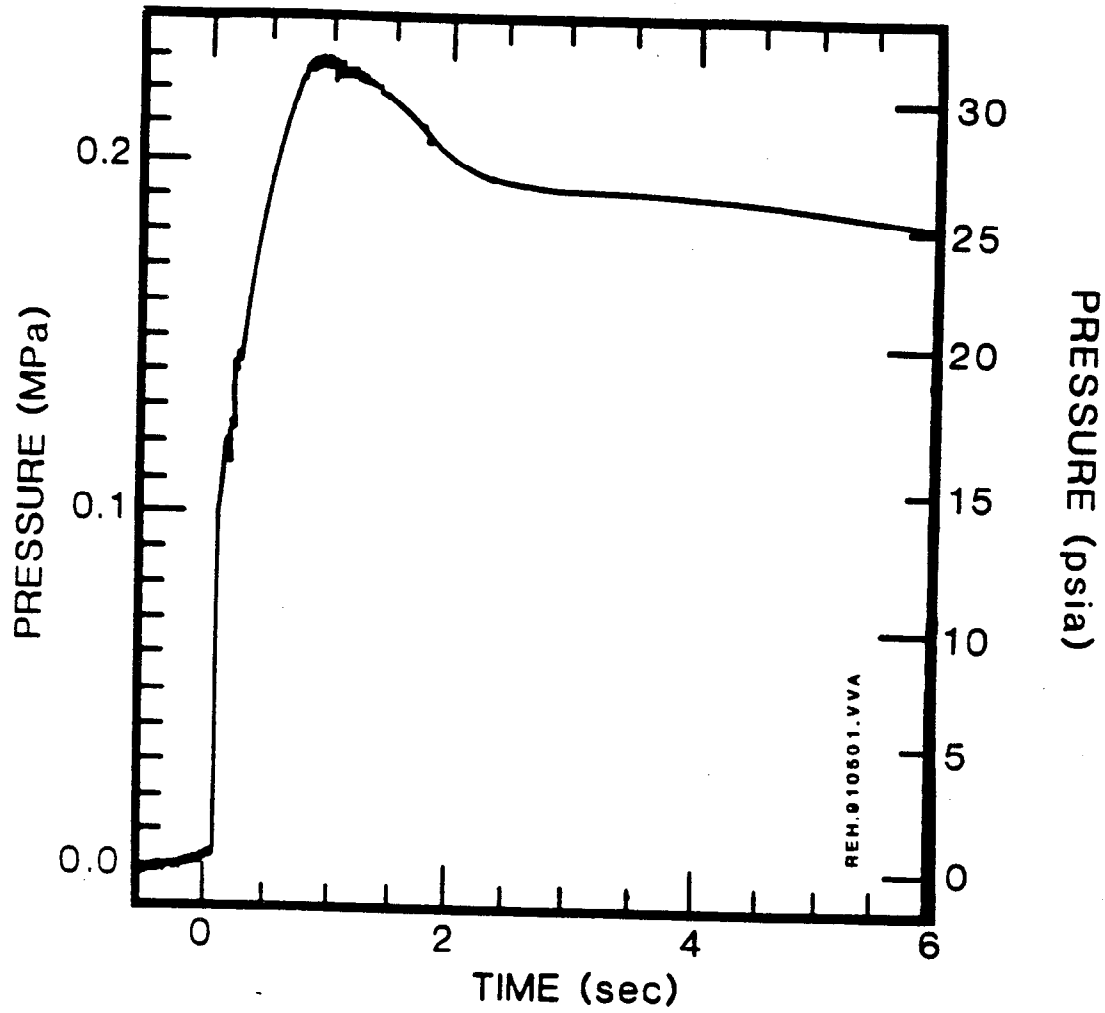


Figure 3-3 FITS2B chamber air pressure.

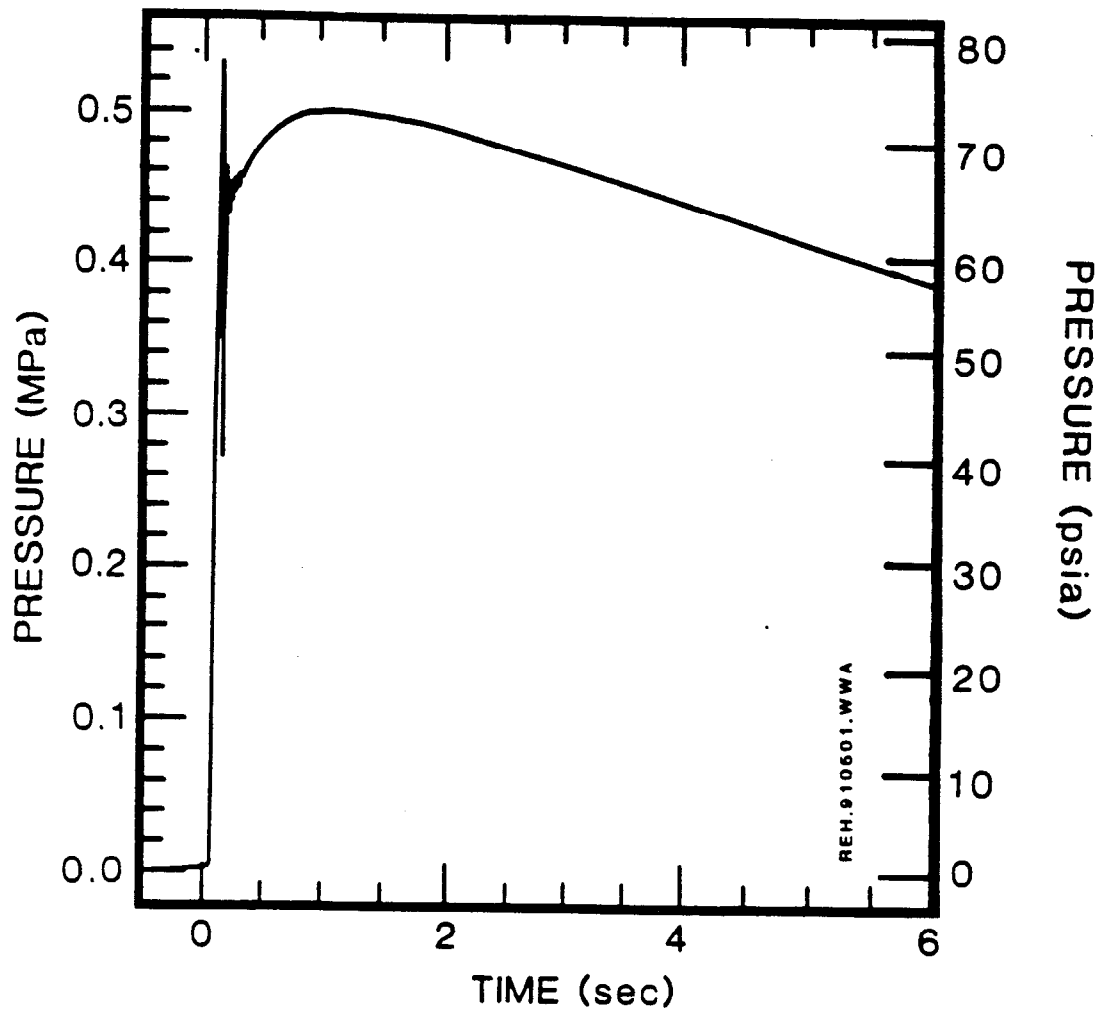


Figure 3-4 FITS3B chamber air pressure.

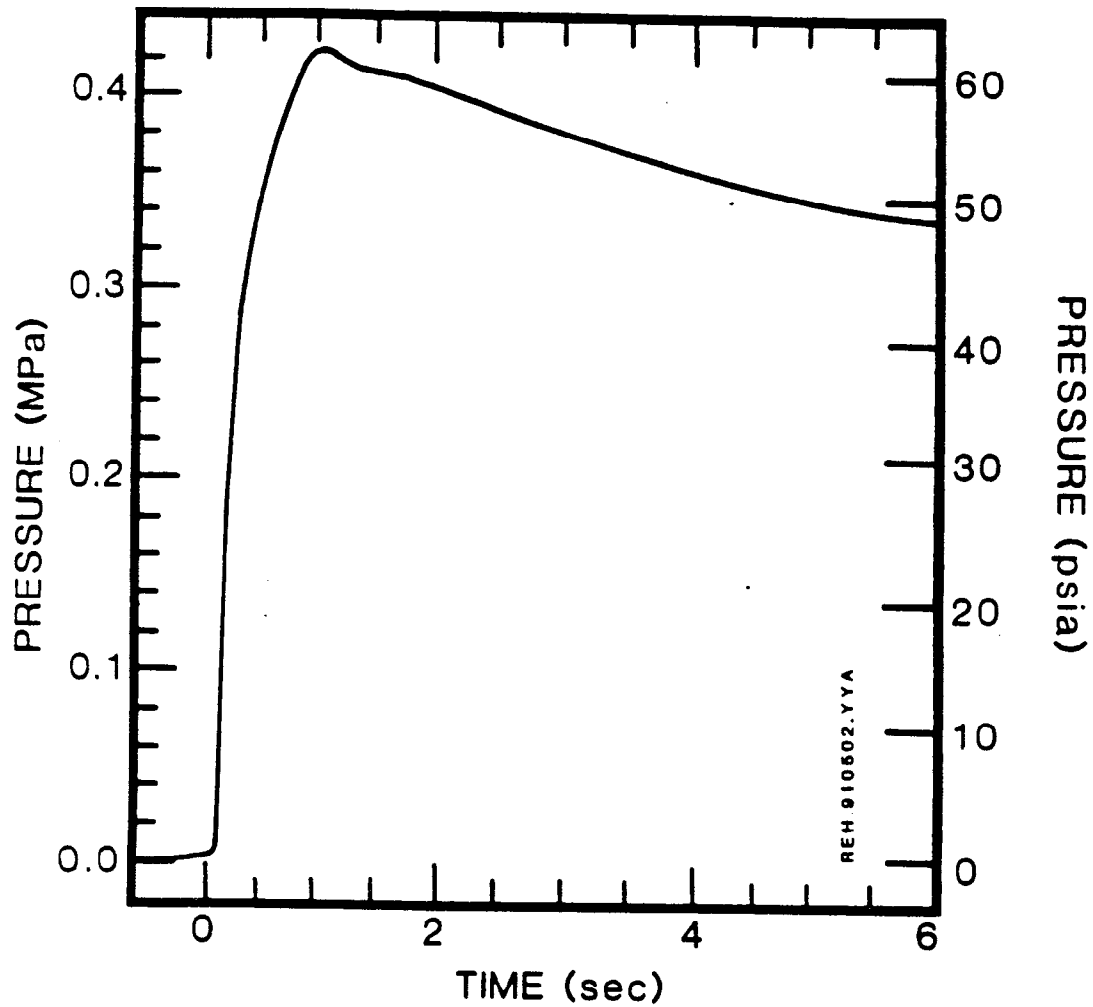


Figure 3-5 FITS6B chamber air pressure (saturated water).

The average steam generation rate can be estimated by using the ideal gas equation.

$$\frac{dP}{dt} = \frac{RT}{V} \frac{dN}{dt} \quad (3-1)$$

where each variable has the standard meaning. As an average representation, assume that the gas space pressure increases 0.35 MPa (51 psi) in 0.5 sec. The volume of the FITS vessel is 198 ft³ (5.6 m³) (Marshall, 1986) and, if an average gas temperature of 260°F (400K) is assumed, the steam generation rate is 2.65 lbm-moles/sec (1.2 kg-moles/sec), which is a mass addition rate of 47.5 lbm/sec (21.6 kg/sec). As the melt enters the vessel, the dynamic interactions (either explosive or non-explosive) would expel melt and water from the lucite test vessel. To provide an equivalent basis for comparison with the FAI/EPRI Mark I tests, the steaming rate should be represented as a heat flux using the cross-sectional area of the FITS vessel (~ 19.4 ft² (1.8 m²)). Using this area, the average heat flux from the melt to the water is about 8.6 x 10⁶ Btu/h-ft² (27 MW/m²), i.e. a value in close agreement with that observed in the Mark I experiments.

3.1.3 Summary

In summary, the results from new, significant scale experiments with greatly different geometries have been compiled to develop a basis on which to provide interpretation for the furnace response due to rapid steam generation by dynamic interactions. Specifically, dynamic interactions should be considered with steam generation rates from 3.2 x 10⁶ to 9.5 x 10⁶ Btu/h-ft² (10 to 30 MW/m²). The projected area of the compartment floor should be used as the pertinent value for determining the total energy production rate. This can then be used to determine if the uncertainties in this range provide for any substantial change in the overall accident evaluation.

3.1.4 Possible Mechanism for Maximum Steam Generation Rate

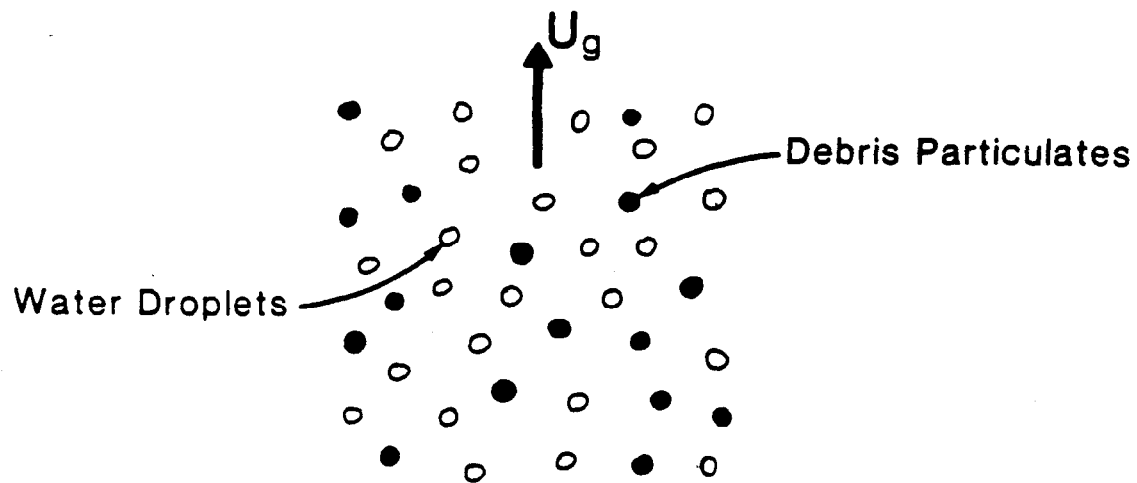
The information presented above was taken from a wide variety of experimental information and provides a substantial data base for describing the maximum melt-water steam generation rate. One can provide a theoretical basis for heat fluxes in the range of 10.4×10^6 Btu/h-ft² (30 MW/m²) for a system with co-dispersed debris and water as depicted in Figure 3-6. A steam velocity sufficient to levitate and separate the water droplets from the high temperature dense debris is given by

$$U_g = \frac{3.7 \sqrt{g\sigma(\rho_f - \rho_g)}}{\sqrt{\rho_g}} \quad (3-2)$$

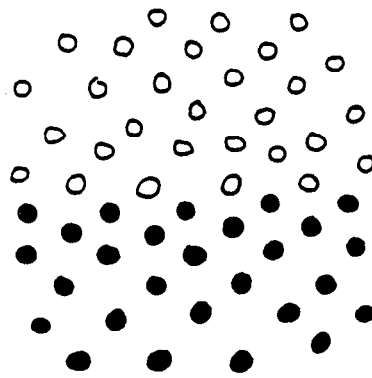
where g is the acceleration of gravity, σ is the steam-water surface tension and ρ_f and ρ_g represent the saturated water and steam densities respectively. If this is considered to be the maximum steam production rate which could exist without separation of the water droplets from the co-disperse configuration, then the heat flux associated with the vapor production rate is given by

$$q/A = 3.7 h_{fg} \sqrt{\rho_g} \sqrt{g\sigma(\rho_f - \rho_g)} \quad (3-3)$$

where h_{fg} is the latent heat of vaporization. Substituting the appropriate values for steam and water at 1 atm into this expression results in a value of 10.4×10^6 Btu/h-ft² (30 MW/m²); a value in agreement with those observed in the various experiments. Hence, the major ramification of an explosive interaction could be the co-dispersion of melt and water which then continues to transfer energy and vaporize water into the atmosphere at a rate limited by the ability of the water droplets to remain as part of the co-dispersed medium.



(a) Co-Dispersed Configuration



(b) Configuration if the Droplets are Fluidized

REL901022 D.B

Figure 3-6 Debris dispersion configuration.

3.1.5 Shock Waves from Steam Explosions

Modeling of the shock waves induced by steam explosions is only necessary if it is conceived that these would challenge the furnace integrity. Figure 3-7 taken from (Glass, 1974) illustrates the decay of substantial shock waves in air as the shock wave expands. A slope corresponding to a pressure amplitude decay proportional to $1/r^2$ is also included for reference and provides a reasonable assessment of the decay characteristic for strong waves. If anything, the higher amplitude portion of the curve decays faster than this simplified representation. If an interaction zone size is postulated along with a maximum pressure for the interaction, this type of decay can be applied to the Sandia FITS experiments to compare the measured shock wave pressures in these tests with this decay characteristic. Table 3-2 summarizes the experimental conditions for the FITSB series, including the size of the test chamber in which the thermite and water were mixed. As an interaction zone, half of the square dimension is used as the radius for the initial calculation. Also, for the peak pressure achieved in the interaction zone one half the critical pressure (~1450 psi or 10 MPa) is used since this corresponds to a condition in which the critical size bubble embryos equal the size for thermally dominated bubble growth (Henry, et al., 1979). For pressures greater than this value, the vapor cannot be produced at a pressure higher than the surrounding ambient. Other experiments have shown this value to be an upper bound of the pressure that can be achieved when the system is not tightly constrained.

The expansion from the interaction zone out to the diameter of the FITS vessel, 2.5 ft (0.76 m) radius, is performed following the approximation shown in Figure 3-7. Since only three different size vessels were used in the eight experiments, only three different shock wave pressures incident on the FITS vessel wall are calculated by this approximate method. These are illustrated in Table 3-3 for the different experiments. As illustrated, this technique substantially overestimates the measured pressure at the FITS vessel boundary. This is not surprising since the curve shown in Figure 3-7 is compared to a chemical explosion which is typically

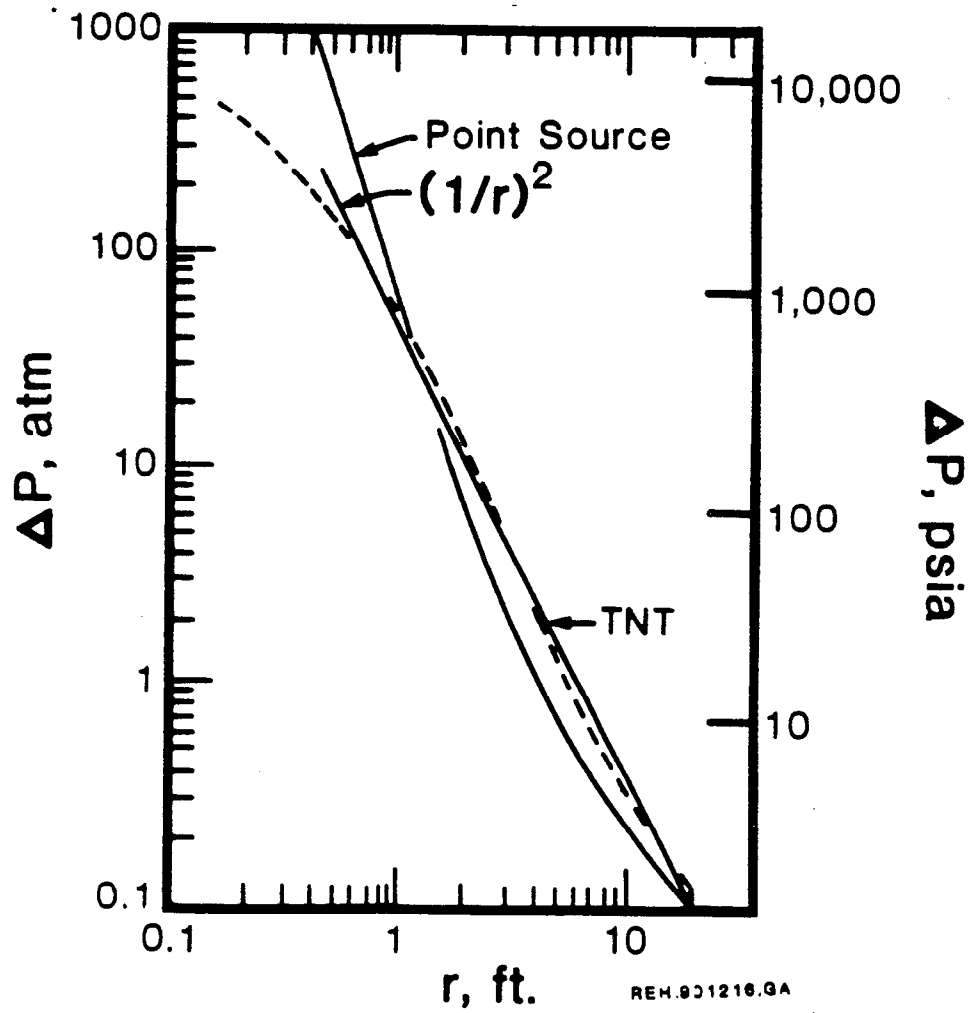


Figure 3-7 Comparison of shock wave pressures for TNT and point source explosions.

Table 3-3

CHAMBER AIR PRESSURE DATA FROM FITSB
(Times From Melt Entry)

Expt.	Steam Explosion Phase				Calculated Pressure Peak (MPa/psig)
	Explosion (s)		Pressure Peaks (MPa/psig)		
	1st ¹	2nd	1st	2nd	
1B	0.144	0.282	0.095/12.78	0.197/28.6	1.6/218
4B	0.029	0.146	0.020/2.9	0.500/72.5	1.6/218
8B	0.017	0.144	0.01/1.45	0.373/54.1	1.6/218
2B	0.087	n.o. ²	0.220/31.9	n.o.	1.6/218
3B	0.081	n.o.	0.440/63.8	n.o.	0.7/87
6B	n.o.	n.o.	n.o.	n.o.	0.9/116
7B	±0.20	n.o.	0.01/1.45	n.o.	0.7/87
9B	0.102	n.o.	0.210/30.45	n.o.	1.6/218

¹ Time taken from start to pressure rise. Zero time taken from average of two active melt position sensors 2.5 cm above water surface.

² Not observed.

more energetic and has a stronger shock wave than those generated by steam explosions.

3.1.6 Metal-Water Reactions During Explosive Interactions

One experiment has been performed in which the high temperature melt dropped into water contained highly reactive metals and measurements were made with respect to the extent of hydrogen formation (Wang, et al., 1989). In these experiments, a thermite fixture representing the fuel material from a light water reactor was dropped into water. As part of the mixture, highly reactive chromium was included and measurements of the subsequent hydrogen formed during the quenching process were made. The experiments typically showed that when the melt was dropped into water, a few percent, perhaps as much as 5%, of the metal was oxidized. This gives a demonstration of the competitive processes between quenching of the high temperature melt and the exothermic oxidation process ongoing at the same time.

3.2 Hydrogen Burns

Numerous experiments have been performed to establish the combustion limits of hydrogen as a function of hydrogen concentration. The generally accepted lower flammability limit for upward flame propagation in air is 4% by volume hydrogen. Horizontal flame propagation can take place with about 6% by volume hydrogen and downward propagation takes place at about 8% by volume hydrogen. The dominant governing process that controls burn completeness in a quiescent environment near the flammability limits is buoyancy-driven flame propagation. If a mixture containing 4% by volume hydrogen is ignited, the flame propagates upward due to buoyancy and an incomplete burn will result unless there is another mechanism for flame propagation. If a mixture is capable of local ignition, preignition turbulence results in more extensive flame propagation and larger burn completeness. Combustion limits have also been shown by experiment to be a function of inert gas concentration. One such study (Benedick, et al., 1984) provided a demonstration of the inerting capabilities of carbon dioxide, the results for these experiments performed in the VGES test vessel at Sandia are illustrated in Figure 3-8, which is taken from

(Benedick, et al., 1984). This also shows the results of other experiments at Lawrence Livermore and Sandia using steam as the inerting material. As shown, the atmosphere becomes inerted at a CO₂ concentration of 52%.

An experimental program was initiated, carried out and analyzed by Westinghouse (Tsai, et al., 1982) to determine the influence of steam in the atmosphere as an inerting medium. The results clearly demonstrated that steam had a strong effect on both the ability to ignite the mixture and the combustion completeness. A correlation was developed for the critical flame temperature to describe the influence of steam. (Critical flame temperature is a means of representing whether the mixture is combustible.)

Another substantial experimental program was performed in the FITS vessel at Sandia to clearly define the combustion boundaries for a hydrogen-air-steam mixture both in quiescent conditions and in a turbulent environment (fans operational). This set of experiments is particularly meaningful to accident management evaluations because (1) steam is the inerting medium, (2) the boundary is clearly defined and (3) the experimental apparatus took great pains to attempt ignition of the mixture. Figure 3-9 taken from (Marshall, 1986) illustrates the test results for the "fans off" state and Figure 3-10, also taken from (Marshall, 1986), depicts the test data for the "fans operational" condition. Those conditions which are represented as "no burn" represent the mixture state in which neither repeated spark initiators nor a glow plug were capable of initiating a burn. Based on these experimental results, it can be concluded that even in the presence of turbulence induced by the accident condition, one still observes steam inerting and well defined flammability limits.

The experimental information was subsequently formulated into a correlation to represent the combustion limits. This is given by

$$\% \text{ Steam} = 100 - \% \text{ H}_2 - 37.3e^{-0.007\% \text{ H}_2} - 518.0e^{-0.488\% \text{ H}_2} \quad (3-4)$$

and is compared to the experimental results in Figure 3-11. Hence, if sufficient steam is released to a non-inerted volume to produce a steam

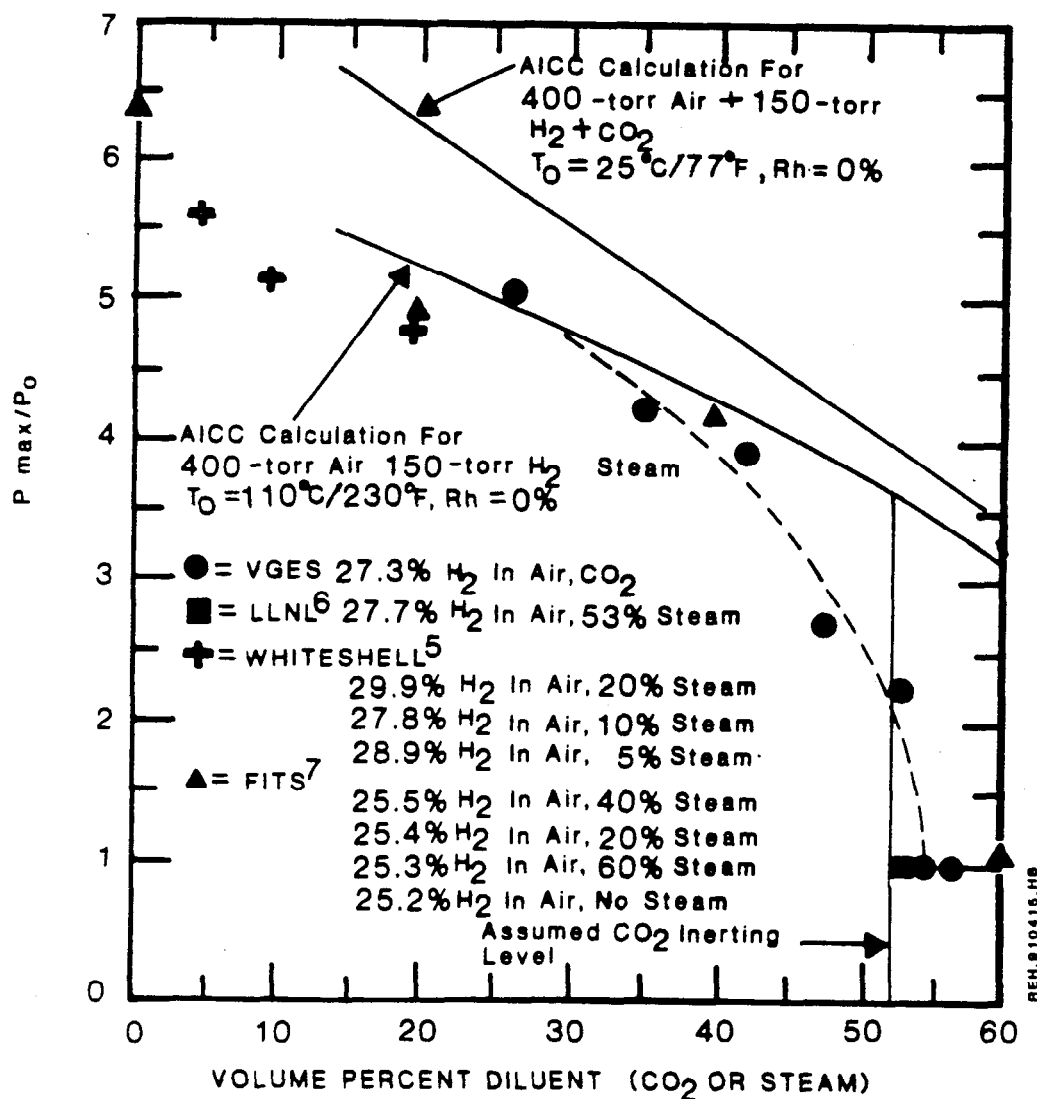


Figure 3-8 Normalized peak pressure (P_{max}/P_0) for hydrogen: air:diluent mixtures, comparing CO_2 and steam (AICC - adiabatic isochoric complete combustion, R_h = relative humidity) (Benedick, 1984).

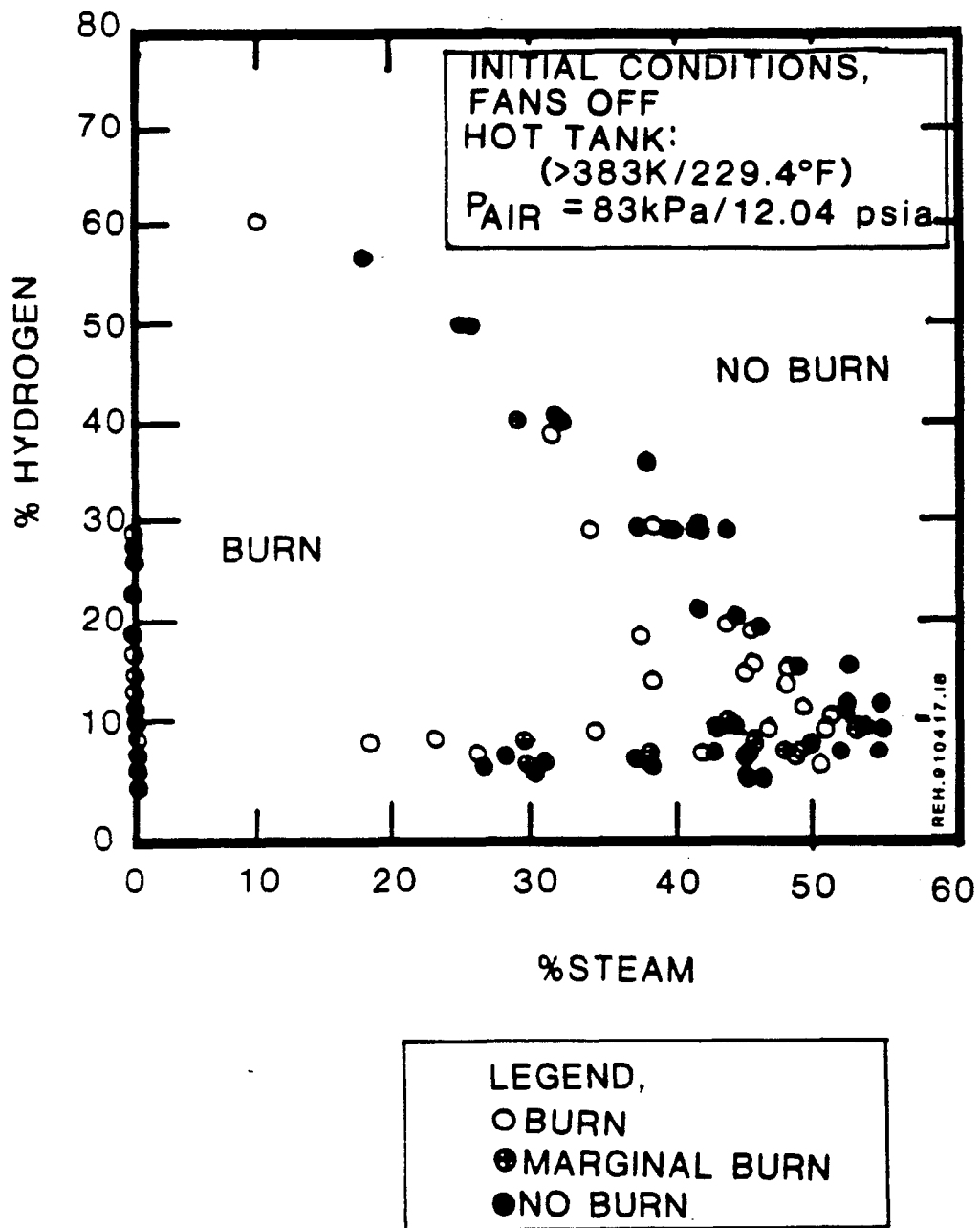


Figure 3-9 Hydrogen:air:steam flammability data with fans off (Marshall, 1986).

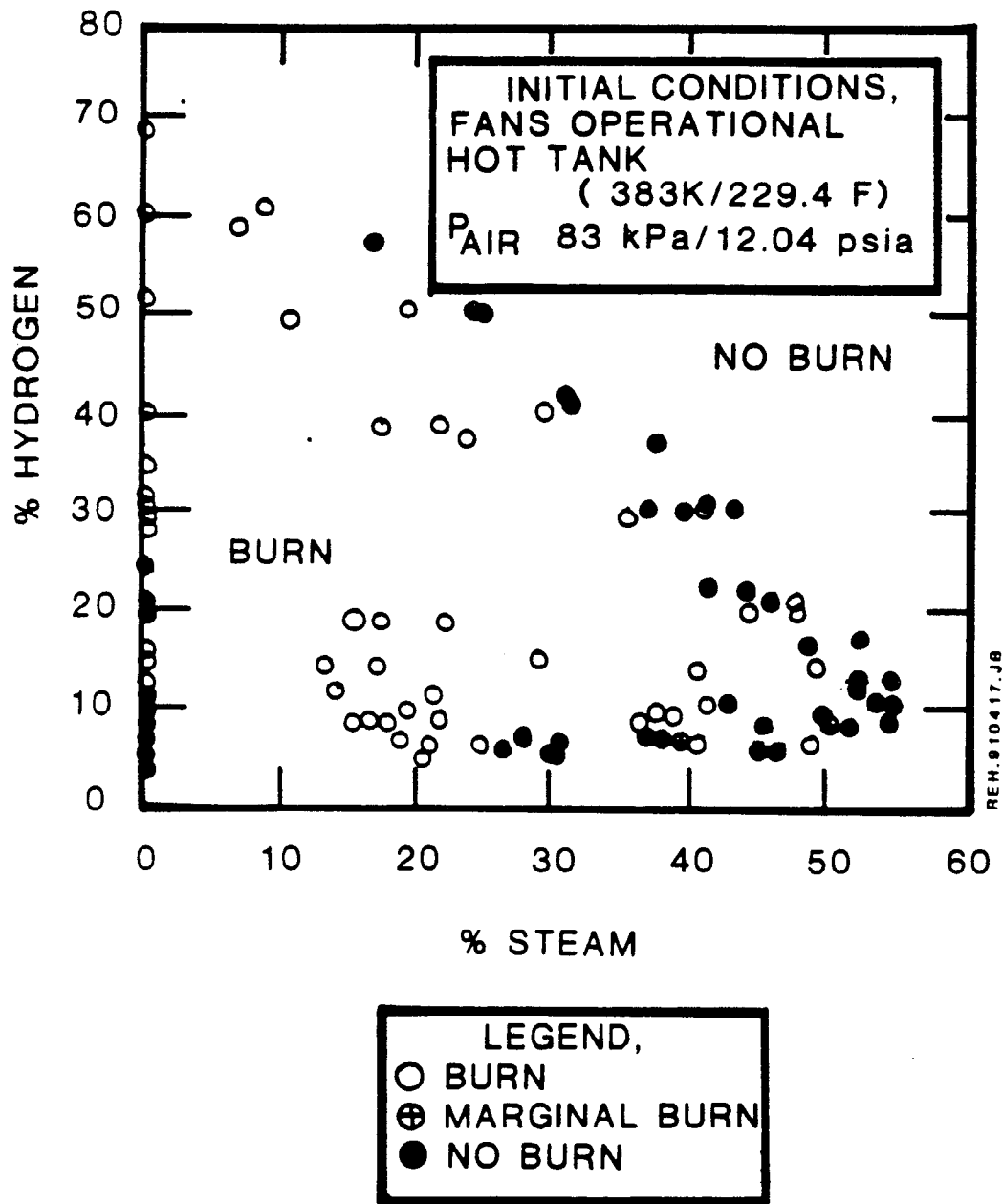


Figure 3-10 Hydrogen:air:steam flammability data with fans operational (Marshall, 1986).

partial pressure of slightly over one atmosphere, hydrogen combustion would be precluded regardless of the hydrogen mass accumulated in the volume.

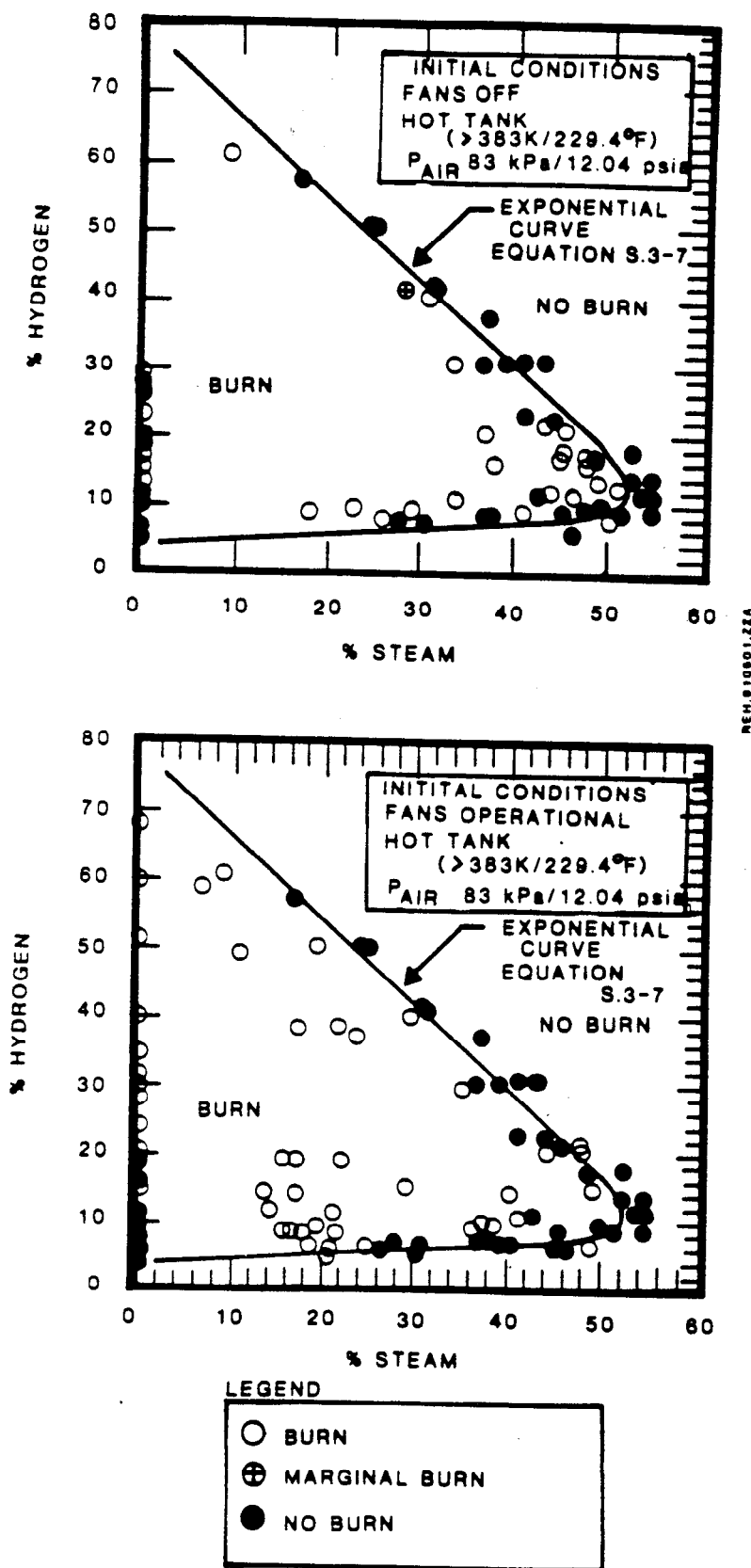


Figure 3-11 Hydrogen:air:steam flammability data with fans on and off shown with the exponential curve fit (Marshall, 1986).

4.0 STEAM EXPLOSION EVALUATION

As discussed in (FAI, 1990a), subcooled coolant conditions are generally required to produce intermixing and explosive interactions for high temperature systems, assuming a sufficient trigger is available. Only in case of multiple failures (as discussed in Section 2.0) where subcooled water may be present as a result of prior pressurization due both to loss of pressure boundary integrity and internal coolant circuit integrity does a potential for intermixing and an explosion occurrence exist. Even in this unlikely event an energetic explosive event can be ruled out as discussed below.

Based upon discussions in Sections 2 and 3, the most likely potential for interaction between the molten uranium metal and the coolant water would appear to be following accumulation of the material within the mold and on the bottom of the vacuum chamber. Given isolation of the cooling coil water as discussed in Section 2, the accumulated water level within the mold would be limited to about 0.06 m and on the floor of the vacuum furnace would be limited to about 0.045 m. It is noted that elevated temperature of the mold would prevent accumulation of subcooled water as vigorous boiling would be experienced as the water tries to enter the mold. The boiling water would prevent any subsequent energetic thermal interaction with the molten metal. Assuming heatup of the mold prior to establishing molten metal condition should therefore be considered as part of the operating procedures.

Furthermore, the shallow layers of water would not allow the necessary pre-mixing configuration to be established between the molten metal and the water, a prerequisite of energetic interactions. This can be illustrated by considering the required water pool height required to completely break up a molten metal jet given by (Epstein and Fauske, 1989)

$$L/D = 6.25 \left(\rho_M / \rho_w \right)^{1/2} \quad (4-1)$$

where L (m) = height of water pool or layer,

D (m) - diameter of the molten jet pour,

ρ_M (kg m^{-3}) - density of uranium metal, and

ρ_w (kg m^{-3}) - density of water.

Considering the molten uranium jet pour diameter to be of the same dimension as the crucible stopper rod (~ 0.02 m), we estimate a required breakup length of about 0.5 m, i.e., about an order of magnitude larger than the available water pools (~ 0.05 m). We conclude from the above considerations that the required premixing configuration of molten particles interdispersed in equal volume of the volatile fluid necessary for an energetic interaction, cannot develop. Instead a configuration consisting initially of a molten uranium metal layer and a water layer separated by a steam blanket would likely develop. (We note that instantaneous physical contact between the molten metal and water as the material descend into the mold or onto the bottom of the vacuum chamber, would at the very worst result in violent splashing and no significant pressure generation.) The development of a largely stratified flow regime is known to produce relatively benign thermal interactions involving only a very small fraction of the molten material (Bang and Corradini, 1991).

Given the presence of a timely trigger that would collapse the vapor layer locally while the uranium metal is still molten (note that the metal would cool rapidly due to the presence of the cold and massive vacuum chamber floor - 1 in. steel plate as well as heat removal due to film boiling), the potential for a propagating steam explosion in connection with the initially separated or stratified regime needs to be considered.

For systems which have demonstrated propagating vapor explosions, the corresponding propagation velocity has been observed to be of the order of 100 m/s (Board and Hall, 1976). Since the fragmentation and intermixing velocity cannot exceed the measured propagation velocity, a first order estimate of the time required for fine scale fragmentation of the molten metal and water layers can be obtained from (Bankoff, 1978):

$$\tau = 3 \frac{d}{U} \sqrt{\frac{\rho_M}{\rho_w}} \quad (4-2)$$

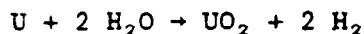
where d is set equal to the thickness of the accumulated molten uranium layer (~ 0.007 m); U is the propagation velocity; and ρ and ρ_c are the uranium metal and water densities, respectively, and results in a fragmentation time of about 10^{-3} s, which is characteristic of thermal explosion time scale.

However, for systems which have demonstrated propagating vapor explosions, T_i is generally well above the critical temperature, while the observed peak shock pressure at the source is well below the critical pressure (Henry, et al., 1976; Henry and Fauske, 1979). The dynamic impact pressure within the liquid ($\rho u a$, where ρ is the liquid density, u is the propagation velocity and a is the velocity of sound in the liquid) resulting from vapor collapse would therefore appear to be the main pressure source for suppressing the retarding effect due to vaporization during the necessary fine scale fragmentation and intermixing process. In view of the limited water layer, the time scale for intermixing becomes extremely small and to a first order is given by d/a . Required time to avoid evaporative forces is therefore of the order of $(0.05/1500) = 10^{-5}$ s which is much smaller than the estimated breakup time, Equation (4-2). It follows that no significant fine scale intermixing can take place, leading to the absence of any damaging steam explosion pressures. As discussed in Section 3, steaming rates resulting from such benign interactions can be enveloped by considering an equivalent surface heat flux of about 30 MW/m^2 .

5.0 HYDROGEN BURN EVALUATION

Given multiple failures (crucible cracking, coolant coil failure and vacuum chamber pressure failure resulting in inflow of air) as discussed in Section 2.0, the possibility of H₂-deflagration also needs to be evaluated.

Consideration of chemical reaction between molten uranium and water and formation of H₂ according to



indicates that oxidation of only about 0.33% of the available uranium (~ 100 kg) would satisfy the lower flammability limit (~ 5%) for H₂ in dry air.* This assumes that H₂ is accumulating in the vacuum chamber (~ 1275 l) as it is being formed, e.g., H₂ is not escaping through the leak(s) or vents as it is being formed. However, as discussed in Section 3, the presence of inert steam material in the vacuum chamber will have a significant effect on the potential as well as the severity of a H₂-deflagration. The presence of steam in excess of 50% volume percent in the vacuum chamber eliminates the deflagration potential altogether independent of H₂ concentration.

The rate equation for metal oxidation in the temperature range of interest is given by (Baker, 1983)

*The required quantity of steam to oxidize 0.33 kg of uranium is about 0.05 kg. While this quantity is much smaller than the quantity of water assumed available (~ 10 gallons) in the multiple failure scenario, it is well above the water vapor quantity that would result if the vacuum chamber were to be filled by ambient air as a result of a broken viewport (assuming 100% relative humidity, the water vapor quantity would be limited to about 0.02 kg). Furthermore, in the case of an intact vacuum chamber, a small but steady water leak could oxidize uranium but would not result in a damaging mixture due to lack of oxidizer (i.e., air).

$$w^2 = 7.5 \cdot 10^5 t \exp(-25,000/RT) \quad (5-1)$$

where w (mg/cm²) = amount of metal oxidation per unit area for a specified time,

t (s) = duration of metal oxidation,

R (cal/g-mole-K) = gas constant (1.987), and

T (K) = metal temperature (~ 1773K).

Considering the extreme case of setting the exposed metal surface area equal to the maximum possible metal pool surface area of 0.84 m² or 8365 cm² and the metal temperature equal to 1500°C or 1773K, Equation (5-1) suggests a time interval of $t \approx 2.6$ s to oxidize enough metal ($w \approx 40$ mg/cm²) to satisfy the lower flammability limit (~ 5%) for H₂ assuming dry air.

A lower bound steaming rate can be evaluated assuming film boiling where the heat flux is given by

$$q \approx \sigma(T_M^4 - T_s^4) + h_c(T_M - T_s) \quad (5-2)$$

where q (W m⁻²) = film boiling heat flux,

σ (W m⁻² K⁻⁴) = Stefan-Boltzman constant ($5.65 \cdot 10^{-8}$),

T_M (K) = uranium metal temperature (~ 1773K),

T_s (K) = steam saturation temperature (~ 373K),

h (W m⁻² K⁻¹) = film boiling convection heat transfer coefficient (~ 100 W m⁻² K),

and results in a heat flux of about ~ 700,000 W m⁻². The above heat flux gives rise to a steaming rate of about 0.26 kg s⁻¹ based upon a pool surface area of about 0.84 m².

Recalling the time interval to oxidize enough metal to reach the lower flammability limit of H₂ in dry air of about 2.6 s, results in about 0.7 kg

of steam. This is equivalent to about 37.6 g-moles or 842 l which translates to about 66 volume percent of steam in the vacuum chamber. (Note that less than 10% of the steam production is enough to satisfy metal oxidation.)

It follows from the above considerations and the discussion provided in Section 3, that sufficient steam inerting will take place in the vacuum chamber for the postulated accident scenarios to eliminate the potential for H₂ deflagration.

6.0 RELIEF REQUIREMENTS

Given isolation of the cooling coil water in case of leakage as discussed in Section 3.0, the accumulated water level on the floor of the vacuum furnace is limited to about 0.045 m. Considering the shallow water pool, a very conservative estimate of the steaming rate resulting from interaction between molten uranium dripping into the water located on the floor of the vacuum chamber is estimated to be about 11 kg s^{-1} .^{*} This value results from using the peak experimental heat flux value of 30 MW m^{-2} and the maximum possible pool surface area of 0.84 m^2 , which is an area consistent with the manner in which the heat flux information was developed (as discussed in Section 3.0). A vaporization rate in excess of about 11 kg s^{-1} , would result in fluidization and separation of the water from the molten uranium and cutoff of the heat transfer.

In the absence of venting an upper bound value for the subject pressure transient in connection with a postulated molten uranium metal-water interaction on the floor of the vacuum chamber can be estimated from

$$\frac{dP}{dt} = \frac{RT}{V} \frac{dN}{dt} \quad (6-1)$$

where P (Pa) = pressure in the vacuum chamber,

t (s) = time,

R ($\text{J kg-mol}^{-1} \text{ K}^{-1}$) = gas constant (8,314),

T (K) = temperature (~ 400K),

V (m^3) = volume of vacuum chamber (~ 1.28 m^3), and

dN/dt (kg-mol s^{-1}) = steaming rate.

^{*}Consideration of molten uranium-water interaction in the mold assembly leads to a steaming rate of 1.73 kg s^{-1} .

Considering the interaction between molten uranium metal gives rise to a maximum steaming rate of about 11 kg s^{-1} ($\sim .61 \text{ kg-mol s}^{-1}$), Equation (6-1) can be integrated to give

$$P = \frac{(8.314)(400)}{(1.28)} (.61)t$$

$$= 1.59 \cdot 10^6 t \quad (6-2)$$

Considering multiple failures including loss of vacuum pressure prior to interaction (worst case), Equation (6-2) suggests that the design pressure of 15 psig ($\sim 1.03 \cdot 10^6 \text{ Pa}$) is reached in about 0.065 s. In case of intact pressure boundary at the time of the molten uranium-water interaction, this time is increased to about 0.12 s.

A sustained steaming rate of about 11 kg s^{-1} would result in complete absorption of the sensible heat from 100 kg of molten uranium in about 1 second. In the absence of venting and neglecting heat losses, Equation (6-2) suggests an upper bound value of the pressure buildup of about 230 psi.

The necessary relief area, A, to safely vent the above steaming rate at the design pressure of 15 psig, can be estimated from

$$W_g = \eta \rho_{g_0} A u_{sv} \quad (6-3)$$

where W_g (kg s^{-1}) is the steaming rate ($\sim 11 \text{ kg s}^{-1}$), η is the critical pressure ratio (~ 0.55), ρ_{g_0} is the steam density at the stagnation pressure ($\sim 1.2 \text{ kg m}^{-3}$), and u_{sv} is the sonic velocity of steam ($\sim 500 \text{ m s}^{-1}$). The above parameter values lead to a relief area requirement of about 0.033 m^2 suggesting that two 6-inch ports would be adequate without causing the pressure buildup to exceed the design pressure of 15 psig.

It is noted that the venting arrangement and design (duct plus filter, etc.) external to the vacuum chamber is considered outside the scope of

this study. For this purpose the arrangement should be designed to accommodate a conservative steaming rate of about 11 kg s^{-1} .

Recalling that two 6-inch fully open ports would be adequate to vent a steaming rate of about 11 kg s^{-1} without causing the pressure buildup to exceed the design pressure of 15 psig the above considerations suggest that the opening pressure for the relief system should be set near ambient pressure ($\sim 1 \text{ psig}$) to allow for the maximum time ($\sim 0.1 \text{ s}$) to assure a fully open relief system as the pressure approaches the design pressure of 15 psig.

7.0 OPERATIONAL CONSIDERATIONS

With the operating philosophy to limit the potential for interactions between the molten uranium and water, there are several aspects of the system design which should be considered. These are listed below.

1. The system should not have power supplied to the furnace induction coils to melt the uranium until the mold has been preheated to 800°C. This preheated state would eliminate any trace water imbedded in the surface cavities within the mold and prevent localized interactions which would cause splattering and would prevent any unknown state of water resident in the mold which could promote explosive interactions.
2. If a coolant line on any of the three systems were to fail, there is no way to cause a substantial interaction between the water and the molten uranium if the melt is held within the crucible. Therefore, the operating philosophy should be to isolate the coolant flow to the induction coils and freeze the molten uranium within the crucible if there is any indication of an accident condition. The crucible cannot be harmed by turning off the power and stopping the coolant flow to the induction coils. In essence this implies that any condition which detects a loss of vacuum should shutdown the heating and cooling to the induction coils and allow the melt to freeze in the crucible.
3. Since the crucible and the mold are installed in the furnace as two separate entities, an interlock should be installed between the mold and the crucible which ensures that the desired relative position of these two elements is correct before power is applied to the mold which precedes the heating of the crucible. This interlock would minimize the chance of any spillage of molten uranium metal outside of the mold.
4. It is also recommended that manual shut-off valves be used to back up the automatic shut-off valves in the water circuits. This would assure isolation of the water coolant lines in any condition in which a loss of vacuum is experienced.
5. Maintaining the melt within the crucible would also minimize any potential for hydrogen generation as a result of melt-water interaction.

8.0 THERMAL MELT-THROUGH CONSIDERATIONS

The accumulation of the entire uranium inventory of about 100 kg on the vacuum chamber floor would not lead to melt-through.*

The flat bottom configuration and the low viscosity of the high temperature uranium metal would result in quick spreading until the metal would freeze, resulting in a layer thickness of only about 0.007 m.

Considering the large heat capacity associated with the 1-inch stainless steel floor panel, we estimate an equilibrium temperature between the uranium metal and the steel plate of only about 250°C, ignoring all other heat loss mechanisms.

*Assuming that the molten uranium metal at a temperature of 1500°C would come into direct contact with the cold stainless steel vacuum chamber floor, a contact temperature of about 750°C is estimated utilizing Equation (2-1), where stainless steel properties have been substituted for the water properties. Since this temperature is less than the eutectic temperature for the uranium metal-steel system (~ 800°C, Walker, et al., 1975), significant wall attack by eutectic formation can be ruled out. Substantial heat losses including quenching by the presence of water would further eliminate any concerns related to thermal melt-through.

9.0 SUMMARY AND CONCLUSIONS

Based upon the above considerations the following conclusions can be made:

- Damaging shock pressures resulting from possible explosive (steam) interaction between molten uranium ($\sim 1500^{\circ}\text{C}$) and water can be ruled out due to lack of sufficient premixing between the molten metal and water. Given isolation of the cooling coil water in case of leakage the accumulated water levels within the uranium mold or on the floor of the vacuum furnace is limited to about 0.06 m and 0.045 m, respectively. The limited water layer suggests an acoustic relief time of about 10^{-5} s, which is much less than the required fragmentation time of about 10^{-3} s.
- Considering the shallow water pools, a conservative estimate of the steaming rate resulting from interaction between molten uranium jetting into the water located on the floor of the vacuum chamber is estimated to be about 11 kg s^{-1} . A vaporization rate in excess of this magnitude, would result in fluidization of the water considering the entire floor area of 0.84 m^2 is available for vapor escape (e.g., steaming rate in excess of about 11 kg s^{-1} would separate the water from the molten uranium resulting in cutoff of the heat transfer). The above steaming rate can be accommodated by 2 six-inch ports without causing the pressure buildup to exceed the design pressure of 15 psig.

It is noted that the venting arrangement and design (duct plus filter, etc.) external to the vacuum chamber is considered outside the scope of this study. For this purpose the arrangement should be designed to accommodate a steaming rate of about 11 kg s^{-1} . The relief system should be set near ambient pressure (~ 1 psig) to allow for the maximum time (~ 0.1 s) to

assure a fully open relief system as the pressure approaches the design pressure of 15 psig.

- Given multiple failures (crucible cracking, coolant coil failure and vacuum chamber pressure failure resulting in inflow of air), the possibility of H_2 -deflagration also needs to be evaluated. Consideration of chemical reaction between molten uranium and water and formation of H_2 , indicates that oxidation of only about 0.33% of the available uranium (~ 100 kg) would satisfy the lower flammability limit (~ 5%) for H_2 in dry air. This assumes that the H_2 is accumulating in the vacuum chamber as it is being formed, e.g., H_2 is not escaping through the vents as it is being formed. However, it is well established that the presence of steam in excess of 50% volume percent eliminates deflagration altogether independent of H_2 concentration.

Considerations of simultaneous heat transfer and resulting minimum steaming rates consistent with film boiling considerations as well as corresponding oxidation rates, suggest that the steaming rate would always exceed the 50% volume fraction required for eliminating the potential for damaging deflagrations.

In summary, the evaluations suggest that the current vacuum chamber design given a design pressure of about 15 psig and adequate control valves and timing for limiting water accumulation following cooling coil failures, would appear adequate. This conclusion is based on the availability of 2 six-inch ports to assure adequate relief in case of molten uranium-water interactions. Finally, accumulation of the molten uranium (~ 100 kg) on the floor of the vacuum chamber poses no thermal threat, based on heat capacity considerations alone.

10.0 REFERENCES

- Angelini, S., Yuen, W. W. and Theofanous, T. G., 1993, "Premixing-Related Behavior of Steam Explosions", paper presented at the CSNI FCI Specialist Meeting, Santa Barbara, CA.
- Baker, Jr., L., 1983, "An Assessment of Existing Data on Zirconium Oxidation Under Hypothetical Accident Conditions in Light Water Reactors", Argonne National Laboratory Report.
- Bang, K. H. and Corradini, M. L., 1991, "Vapor Explosions in a Stratified Geometry", Nuclear Science and Engineering, 108, pp. 88-108.
- Bankoff, S. G., 1978, "Vapor Explosions: A Critical Review", Proc. 6th Intl. Heat Transfer Conf., Vol. 6, pp. 355-360.
- Benedick, W. B., et al., 1984, "Combustion of Hydrogen: Air Mixtures in the VGES Cylindrical Tank", NUREG/CR-3273, SAND83-1022.
- Board, S. J. and Hall, R. W., 1976, "Recent Advances in Understanding Large Scale Vapor Explosions", Proc. 3rd Specialist Mtg. on Sodium/Fuel Interaction in Fast Reactors, PNC N251 76-12, Vol. 1, Tokyo, Japan, pp. 22-26.
- Epstein, M. and Fauske, H. K., 1989, "The Three Mile Island Unit 2 Core Relocation - Heat Transfer and Mechanism", Nuclear Technology, Vol. 87, 1021-1035.
- Fauske & Associates, Inc. (FAI), 1990a, "Steam Explosion Evaluation for the UDS Process Vessel", Fauske & Associates, Inc. Report No. FAI/90-14 submitted to Lawrence Livermore National Laboratory.
- Fauske & Associates, Inc. (FAI), 1990b, "Influence of Hydrogen Generation and Combustion", Fauske & Associates, Inc. Report No. FAI/90-32 submitted to Lawrence Livermore National Laboratory.
- Fletcher, D. F. and Denham, M. K., 1993, "Validation of the CHYMES Mixing Model", paper presented at the CSNI FCI Specialist Meeting, Santa Barbara, CA.
- Glass, I. I., 1974, Shock Waves and Man, The University of Toronto Press.
- Henry, R. E., et al., 1976, "Vapor Explosions and Simulant Fluids", Proc. Intl. Conf. on Fast Reactor Safety and Related Physics, Chicago, IL, CONF-761001, p. 1862.
- Henry, R. E. and Fauske, H. K., 1979, "Nucleation Processes in Large Scale Vapor Explosions", Trans. ASME, Jr. of Heat Transfer, Vol. 101, pp. 280-287.

- Henry, R. E., Hammersley, R. J. and Klopp, G. T., 1991, "Direct Containment Heating Experiments in a Zion-Like Geometry", AIChE Symp. Series, Heat Transfer, Minneapolis, 1991, 283, Vol. 87, pp. 86-98.
- Kutateladze, S. S., 1972, "Elements of Hydrodynamics of Gas-Liquid Systems", Fluid Mechanics - Soviet Research, Vol. 1, 4, p. 29.
- Malinovic, B., Henry, R. E. and Sehgal, B. R., 1989, "Experiments Relating to Drywell Shell-Core Debris Interactions", Natl. Heat Transfer Conf., Philadelphia, PA, AIChE Symp. Series, Vol. 85, No. 269, pp. 217-222.
- Marshall, Jr., B. W., 1986, "Hydrogen:Air:Steam Flammability Limits and Combustion Characteristics in the FITS Vessel", NUREG/CR-3468, SAND 84-0383.
- Mitchell, D. E. and Evans, N. A., 1986, "Steam Explosion Experiments at Intermediate Scale: FITSB Series", NUREG/CR-3983, SAND 83-1057.
- Tong, L. S., 1965, Boiling Heat Transfer in Two-Phase Flow, John Wiley & Sons, Inc., New York.
- Tsai, S. S., et al., 1982, "Flame Temperature Criteria Tests", Proc. of the 2nd Intl. Conf. on the Impact of Hydrogen and Water Reactor Safety, Albuquerque, New Mexico.
- Walker, C. M., et al., 1975, "U-Pu-Zr Metal Alloy: A Potential Fuel for LMFBRs", ANL-76-20, November.
- Wang, S. K., Blomquist, C. A., Spencer, B. W., McUmber, L. M. and Schneider, J. P., 1989, "Experimental Study of the Fragmentation and Quench Behavior of Corium Melts in Water", Thermal-Hydraulics Division Trans. ANS Winter Meeting, San Francisco, CA, pp. 26-30.

Appendix B

**Closure on Fauske & Associates, Inc.
Safety Analysis for the Uranium Vacuum Induction Furnace**

Interdepartmental Letterhead

Mail Station L-113


Ext: 2-8569

Fax: 2-5397

CODTU-93-0175
ENDT-93-006
Page 81

**NUCLEAR TEST ENGINEERING DIVISION
Thermo-Fluids Mechanics Group
TFG93-037**

June 29, 1993

TO: John Sze
FROM: C. S. Landram 
SUBJECT: Closure on Fauske & Associates, Inc., Safety Analysis for the
Uranium Vacuum Induction Furnace

Refs.

1. Fauske & Associates, Inc. Safety Analysis, FAI/93-35, June 1993
2. Memo C. S. Landram to J. Sze, "Postulated Break of Ceramic Crucible and Liner for U-Casting Project," TF93-6, February 1, 1993.

The only major difference between the conclusions reached in the Fauske safety analysis (Ref. 1) and those in my work (Ref. 2) is the likelihood of a coolant water line rupture when significant quantities of molten uranium are available to contact the cooling coils following a ceramic crucible breakage. Ref. 1 concludes that the rupture is unlikely, while Ref. 2 concludes, to the contrary, that it is likely. This contradiction is addressed as issue 1 in the accompanying discussion. Because the consequences of a ruptured water line are shown in Ref. 1 to be nil with the engineered safety system design for the apparatus, the contradiction has no particular safety impact.

A minor second issue is in the margin of safety for a potential uranium melt through on the floor of the chamber. In the accompanying computation called issue 2, I show here that the chamber wall never comes close to a melt-through, while Ref. 1 shows that while the melt-through does not occur, the wall temperature nearly approaches the melt temperature. The discrepancy has no safety impact because both calculations show that a melt-through will not occur.

c: W. Comfort
L. Sedlacek

University of California

 **Lawrence Livermore
National Laboratory**

First Issue: Likelihood of a Coolant Coil Rupture (Section 2)

As correctly stated in Ref. 1, the use of equation (2-1) applies prior to the thermal wave penetrating the copper wall thickness (see second paragraph of p. 2-11). This penetration occurs in about .023 msec, after which the trivially thin crust formed (about .002 inch) in the uranium melts almost instantaneously. The heat flux (Ref. 1, last paragraph of p. 2-11) would then not really be limited by crust conduction as stated in Ref. 1 (same paragraph). Rather, as computed in Ref. 2 (p.4), the copper wall will attain the coolant saturation temperature in about 5 msec, and the critical heat flux is exceeded some 1.2 msec later (6.2 msec following the initial contact of uranium and copper tube). Once the critical heat flux is exceeded, the tubing will rupture. The footnote in Ref. 1 (p. 2-11) is very appropriate, and consequently, then, no credit for nucleate boiling should be taken, which then would mean tube rupture occurs sooner – in slightly more than 5 msec (i.e., the additional time of 1.2 msec for nucleate boiling can not be credited).

Because of the above analysis and previous actual observations that such coolant tubes do in fact rupture on contact with uranium, the statement on the middle of p. 2-10 (Ref. 1) is incorrect. It should read: "However, the rupture of the mullite crucible and leakage of uranium onto the water cooled copper tubing used for the reduction coil ~~should not~~ [can likely] result in failure of the induction coil."

It should be recognized that the consequences of a ruptured water line were proven to be nil in Ref. 1. Thus, the fact that a cooling line rupture by melt through is more likely to occur has no impact with respect to a safety issue.

Second Issue: Thermal Floor Melt-Through (Section 8)

As posed on p. 8-1 of Ref. 1, a finite-thick 0.7 cm layer of uranium at 1500° C contacting a 2.54 cm thick stainless steel vacuum chamber floor at 20° C can not be analyzed using Equation (2-1) (with stainless steel properties substituted for copper). Eq. (2-1) is valid only if the two thicknesses were semi-infinite, which of course they are not.

The equilibrium temperature of both finite layers of thickness δ , each having thermal capacitance of $\rho c \delta$, is

$$T(^{\circ}\text{C}) = \frac{(\rho c \delta)_u (1500) + (\rho c \delta)_s (20)}{(\rho c \delta)_u + (\rho c \delta)_s} = 230^{\circ}\text{C}$$

Because the stainless steel will rise to 230° C, it is always well below the 800° C melt-through temperature and well below the 750° C erroneously calculated on p. 8-1 of Ref. 1.